(12) INTERNATIONAL APPLICATION PUBLISHED UNDER THE PATENT COOPERATION TREATY (PCT)

(19) World Intellectual Property Organization
International Bureau

(43) International Publication Date
29 April 2004 (29.04.2004)

PCT

(10) International Publication Number
WO 2004/036176 A2

(51) International Patent Classification[7]: G01N

(21) International Application Number: PCT/US2003/032581

(22) International Filing Date: 16 October 2003 (16.10.2003)

(25) Filing Language: English

(26) Publication Language: English

(30) Priority Data:
60/418,359 16 October 2002 (16.10.2002) US

(71) Applicant (*for all designated States except US*): **DUKE UNIVERSITY** [US/US]; 230 North Building, Research Drive, Box 90083, Durham, NC 27708-0083 (US).

(72) Inventors; and

(75) Inventors/Applicants (*for US only*): **HELLINGA, Homme, W.** [GB/US]; 5212 Pine Cone Lane, Durham, NC 27705 (US). **LOOGER, Loren, L.** [US/US]; 128 Scenic Drive, Madison, AL 35758 (US).

(74) Agent: **TANIGAWA, Gary, R.**; Nixon & Vanderhye P.C., 1100 North Glebe Road, Suite 800, Arlington, VA 22201-4714 (US).

(81) Designated States (*national*): AE, AG, AL, AM, AT, AU, AZ, BA, BB, BG, BR, BY, BZ, CA, CH, CN, CO, CR, CU, CZ, DE, DK, DM, DZ, EC, EE, EG, ES, FI, GB, GD, GE, GH, GM, HR, HU, ID, IL, IN, IS, JP, KE, KG, KP, KR, KZ, LC, LK, LR, LS, LT, LU, LV, MA, MD, MG, MK, MN, MW, MX, MZ, NI, NO, NZ, OM, PG, PH, PL, PT, RO, RU, SC, SD, SE, SG, SK, SL, SY, TJ, TM, TN, TR, TT, TZ, UA, UG, US, UZ, VC, VN, YU, ZA, ZM, ZW.

(84) Designated States (*regional*): ARIPO patent (GH, GM, KE, LS, MW, MZ, SD, SL, SZ, TZ, UG, ZM, ZW), Eurasian patent (AM, AZ, BY, KG, KZ, MD, RU, TJ, TM), European patent (AT, BE, BG, CH, CY, CZ, DE, DK, EE, ES, FI, FR, GB, GR, HU, IE, IT, LU, MC, NL, PT, RO, SE, SI, SK, TR), OAPI patent (BF, BJ, CF, CG, CI, CM, GA, GN, GQ, GW, ML, MR, NE, SN, TD, TG).

Published:
— *without international search report and to be republished upon receipt of that report*

For two-letter codes and other abbreviations, refer to the "Guidance Notes on Codes and Abbreviations" appearing at the beginning of each regular issue of the PCT Gazette.

(54) Title: BIOSENSOR

(57) Abstract: Biosensors are made by attaching covalently or non-covalently at least one reporter group to one or more specific positions of a bacterial periplasmic binding protein (bPBP). Upon binding of ligand to the biosensor, there is a change in the signal transduced by the reporter group.

WO 2004/036176 A2

BIOSENSOR

CROSS-REFERENCE TO RELATED APPLICATIONS

This application claims the benefit of provisional Appln. No. 60/418,359, filed October 16, 2002.

FEDERALLY SUPPORTED RESEARCH OR DEVELOPMENT

The U.S. Government has certain rights in this invention as provided for by the terms of NIH-RO1-GM49871 and ONR-N00014-98-1-0110.

TECHNICAL FIELD

The present invention relates to biosensors and to methods of making and using same.

BACKGROUND

Biosensors are analytical tools that can be used to measure the presence of a single molecular species in a complex mixture by combining the exquisite molecular recognition properties of biological macromolecules with signal transduction mechanisms that couple ligand binding to readily detectable physical changes (Hall, *Biosensors*, Prentice-Hall, Englewood Cliffs, New Jersey; Scheller et al., Curr. Op. Biotech. 12:35-40, 2001). Ideally, a biosensor is reagentless and, in contrast to enzyme-based assays or competitive immunoassays, does not change composition as a consequence of making the measurement (Hellinga & Marvin, Trends Biotech. 16:183-189, 1998). Most biosensors combine a naturally occurring macromolecule such as an enzyme or an antibody, with the identification of a suitable physical signal particular to the molecule in question, and the construction of a detector specific to that system (Meadows, Adv. Drug Deliv. Rev. 21:177-189, 1996). Recently, molecular engineering techniques have been explored to develop macromolecules that combine a wide range of binding specificities and affinities with a common signal transduction mechanism, to construct a generic detection system for many different analytes (Hellinga & Marvin, Trends Biotech. 16:183-189, 1998).

Escherichia coli periplasmic binding proteins are members of a protein superfamily (bacterial periplasmic binding proteins, bPBPs) (Tam & Saier, Microbiol. Rev. 57:320-346, 1993) that has been shown to be well suited for the engineering of biosensors (U.S. Patent 6,277,627). These proteins comprise two domains linked by a hinge region (Quiocho & Ledvina, Molec. Microbiol. 20:17-25, 1996). The ligand-binding site is located at the interface between the two domains. The proteins typically adopt two conformations: a ligand-free open form, and a ligand-bound closed form, which interconvert via a hinge-bending mechanism upon ligand binding. This global, ligand-mediated conformational change has been exploited to couple ligand binding to changes in fluorescence intensity by positioning single, environmentally sensitive fluorophores in locations that undergo local conformational changes in concert with the global change (Brune et al., Biochemistry 33:8262-8271, 1994; Gilardi et al., Prot. Eng. 10:479-486, 1997; Gilardi et al., Anal. Chem. 66:3840-3847, 1994; Marvin et al., Proc. Natl. Acad. Sci. USA 94:4366-4371, 1997, Marvin and Hellinga, J. Am. Chem. Soc. 120:7-11, 1998; Tolosa et al., Anal. Biochem. 267:114-120, 1999; Dattelbaum & Lakowicz, Anal. Biochem. 291:89-95, 2001; Marvin & Hellinga, Proc. Natl. Acad. Sci. USA 98:4955-4960, 2001; Salins et al., Anal. Biochem. 294:19-26, 2001). Conformational coupling mechanisms can also be devised to alter the flow of current between the surface of an electrode derivatized with the engineered bPBP containing a covalently attached redox cofactor (Benson et al., Science 293:1641-1644, 2001).

The present invention provides a method of utilizing bPBPs to generate biosensors for a variety of chemical classes including sugars, amino acids, dipeptides, cations, and anions. These biosensors have widespread utility including in clinical, industrial, and environmental settings.

SUMMARY OF THE INVENTION

The present invention relates to biosensors, making them from mutant or wildtype members of the bacterial periplasmic binding protein (bPBP) superfamily, and using them to assay for (i.e., detect and/or quantitate) ligand. The tertiary structure of bPBPs is comprised of two domains linked by a hinge region with a ligand-binding pocket located at an interface between the two domains. They typically adopt two conformations: a ligand-free open form and a ligand-bound closed form, which interconvert via a hinge-

bending mechanism which depends on whether ligand is bound or not at the site. Biosensors are made by covalently or non-covalently attaching at least one reporter group to one or more specific positions of a bPBP. Upon binding of ligand to the biosensor, there is a change in the signal transduced by the reporter group which can be analyzed by assessing any of its observable properties (e.g., optical or electrochemical properties). Biosensors are classified according to the relationship between the attachment site of the reporter group and the binding site(s) of the ligand (i.e., allosteric, endosteric, or peristeric) or distance between those sites (i.e., distal or proximal).

In accordance with the invention, the event of ligand binding to biosensor changes the local environment of the position-specific attached reporter group. The signal of the reporter group may be generated by one or more fluorophores and/or redox cofactors. The biosensor may be operated under physiological conditions without additional reagents.

Objects and advantages of the present invention will be clear from the description that follows.

BRIEF DESCRIPTIONS OF THE DRAWINGS

Figure 1 shows the 3-D structures of eleven bPBPs indicating locations of allosteric, endosteric, and peristeric sites used. Each protein is shown in the closed form, with bound ligand indicated by ball-and-stick structures. The two domains of each bPBP are oriented vertically with the first (containing the N-terminus) above the second (containing the C-terminus). A hinge segment connects the domains. The structure of histidine BP is used to represent the as yet unsolved structure of glutamate/aspartate BP. Residues mutated to cysteine are indicated by differently shaded spheres, and differentiated as allosteric (heavy shading), endosteric (medium shading, in GBP only), or peristeric (light shading). Structures are grouped by cluster as defined by Tam & Saier (Microbiol. Rev. 57:320-346, 1993) according to sequence-based relationships. Cluster 2: arabinose BP (ABP), glucose BP (GBP), and ribose BP (RBP). Cluster 5: dipeptide BP (DPP). Cluster 3: glutamine BP (QBP), histidine BP (HBP), and glutamate/aspartate BP (EBP). Cluster 6: phosphate BP (PBP) and sulfate BP (SBP). Cluster 1: maltose BP (MBP) and Fe(III) BP (FeBP). Molecular graphics were rendered with Molscript (Kraulis, J. Appl. Crystallogr. 24:946-950, 1991).

Figure 2, shows alignment of sequences of *E. coli* YBEJ (putative glutamate/ aspartate BP), glutamine BP, and histidine BP using clustalW (Thompson et al., Nucl. Acids Res. 22:4673-4680, 1994). Numbering begins from the putative initiation codon of the open reading frame for YBEJ, including its leader sequence. The underlined methionine is the initiation codon for expression of YBEJ used in the study. Residues in each protein that were mutated to cysteine for fluorophore conjugation are in bold font. The letters "a" and "p" beneath these residues indicate their classification as allosteric or peristeric, respectively.

Figure 3 shows structural formulae of thiol-reactive fluorophores. Approximate wavelengths of maximal fluorescence excitation and emission, respectively, of the protein-bound fluorophores are (in nm): pyrene (340, 390); acrylodan (390, 500); fluorescein (485, 520); NBD (490, 540); NBDE (490, 530); JPW4039 (485, 590); JPW4042 (470, 640); and JPW4045 (470, 640).

Figures 4A and 4B show a definition of fluorimetric parameters. Fig. 4A shows parameters λ_{std}, I_1, and I_2 used to determine the standard intensity change ΔI_{std}. Fig. 4B shows parameters A_1, A_2, $^{\circ}A$, and $^{\infty}A$ used to determine ΔR. Each of the areas $^{\infty}A$ encompasses the respective area $^{\circ}A$.

Figures 5A and 5B show fluorimetric titration of glucose BP and glutamate/ aspartate BP conjugates. Fig. 5A shows titration of glucose BP W183C-acrylodan with glucose. Fig. 5B. Titration of glutamate/aspartate BP T129C-NBD with amino acids. Data points: ● glutamic acid; + aspartic acid; ◆ asparagine; × glutamine. In Fig. 5A and Fig. 5B the lines shown are the best fit binding isotherms.

Figures 6A-6C shows occurrence of fluorimetric parameters in the set of 320 fluorescent conjugates. Fig. 6A shows distribution of the shift in wavelength of maximum fluorescent intensity ($^{max}\lambda_{saturated}$-$^{max}\lambda_{apo}$). Fig. 6B shows distribution of the intensity change parameter ΔI_{std}. Fig. 6C shows distribution of the ratiometric change parameter ΔR_{max}. For each parameter, the upper bound of each interval is indicated.

Figure 7 shows occurrence of changes in ligand affinity among the three classes of fluorophore attachment site. Legend: endosteric sites, filled bars; peristeric sites, hatched bars; allosteric sites, open bars. In the case of arabinose BP, the value for $^{wt}K_d$ is that of the C64A mutant, in which all conjugates were made. Data for dipeptide BP and Fe(III) BP are not included. For the former, the K_d for Gly-Leu dipeptide in the wild-type has not been reported. In the case of Fe(III) BP, the K_d of the unconjugated mutant E57D was not determined. For each interval on the x-axis, the upper bound is indicated. For example, the interval labeled "0" contains values of $\log(^{mut}K_d/^{wt}K_d) > -1$ and ≤ 0.

Figures 8A and 8B show ratiometric titration of bPBP fluorophore conjugates using different pairs of emission wavelength bands. Fig. 8A shows glucose BP-W183C conjugated to acrylodan, titrated with glucose at the following ratios of fluorescence emission (wavelengths in nm): ◊, $F_{450\text{-}459}/F_{550\text{-}559}$ ($^{app}K_d \sim 5.0$ mM); □, $F_{450\text{-}459}/F_{486\text{-}495}$ ($^{app}K_d \sim 10.4$ mM); O, $F_{472\text{-}481}/F_{450\text{-}459}$ ($^{app}K_d \sim 17.4$ mM). Lines show fit to equation 4. The normal serum glucose range (euglycemia) of 4 to 6 mM is delimited by vertical lines. Fig. 8B shows ribose BP-T135C conjugated to acrylodan, titrated with ribose at the following ratios of fluorescence emission (wavelengths in nm): □, $F_{501\text{-}510}/F_{450\text{-}459}$ ($^{app}K_d \sim 41$ μM); O, $F_{450\text{-}459}/F_{501\text{-}510}$ ($^{app}K_d \sim 254$ μM); ◊, $F_{450\text{-}459}/F_{547\text{-}556}$ ($^{app}K_d \sim 461$ μM).

DETAILED DESCRIPTION OF THE INVENTION

The present invention relates to biosensors constructed using engineered bPBPs, for example, *E. coli* bPBPs. In accordance with the invention, conjugates are constructed that can be used to monitor binding of ligands to bPBPs. Conjugates can be produced by introducing mutations into a bPBP at one or more specific positions in the protein structure where covalently attached reporter groups (e.g., fluorophores or redox cofactors) respond to a conformational change of the bPBP which occurs upon ligand binding. Other methods for covalently or non-covalently attaching at least one reporter group to one or more amino acid residue positions in the primary amino acid sequence of a mutant or wildtype bPBP include: addition or substitution of any activatable crosslinkers, use of designer or non-natural tRNAs, introduction of coordination sites, etc.

The universality of the engineered conformational coupling mechanism in bPBPs is disclosed herein. As described in the Example that follows, ten bPBPs of known structure have been used, and eight different environmentally sensitive fluorophores have been introduced at a variety of locations predicted to link local conformational changes to ligand-mediated hinge-bending motion. Bioinformatics techniques can be used to predict the location of linked sites in bPBPs the structures of which are not known, thereby making it possible to use the large number of paralogs and homologs that have recently been identified in this family by genomic sequencing studies (Blattner et al., Science 277:1453-1474, 1997; Quentin et al., J. Mol. Biol. 287:467-484, 1999). Together with the opportunities of structure-based redesign of ligand-binding specificity (Hellinga & Richards, J. Mol. Biol. 222:763-785, 1991; Marvin & Hellinga, Proc. Natl. Acad. Sci. USA 98:4955-4960, 2001), the Example provided below demonstrates the vast potential of the bPBP superfamily as the basis for a system of biosensors suited to a broad range of applications.

Furthermore, the ligand-binding pocket may be engineered to bind ligands which are not bound by the wild-type bPBP. The ligand-binding site is located at the interface between the bPBP's two domains. Mutating amino acid residues at that interface which are near (i.e., in or around) the binding site of wild-type bPBP may generate new contacts with ligand (e.g., Zn^{++} for MBP) and destroy or alter binding with cognate ligand (e.g., maltose for MBP). This can be used to change the specificity of the ligand-binding pocket. For example, maltose binding protein has been mutated to specifically bind to noncognate ligand: e.g., metal Zn^{++} ion, trinitrotoluene, L-lactate, and serotonin (Marvin & Hellinga, Proc. Natl. Acad. Sci. USA 98:4955-4960, 2001; Looger et al., Nature 423:185-190, 2003; Dwyer et al., Proc. Natl. Acad. Sci. USA 100:11255-11260, 2003). Thus, biosensors which bind noncognate ligand can be made by mutating amino acid residues at the interface of the two bPBP domains to generate a new ligand-binding pocket; ligand bound by such biosensors may not bind to wild-type bPBP.

Other mutations in the bPBP may be made to affect function of the biosensor: e.g., mutations may increase or decrease binding affinity or specificity; enhance or reduce signal transduction; add a new functionality by fusion with another carbohydrate, lipid, or protein domain; improve thermostability or thermolability; introduce a catalytic activity; shorten or lengthen operational life; widen or narrow the conditions for operation; or any

combination thereof. Preferred is mutating amino acid residues at positions of the bPBP where a reporting group is not attached (e.g., at least one missense mutation which is not a cysteine conjugated through a thiol bond to a fluorophore).

In one embodiment, the present invention relates to a method of constructing a reagentless fluorescent biosensor. The method comprises identifying sites on a bPBP that undergo a local conformational change in concert with a ligand-mediated hinge-bending motion. Cysteine residues can be introduced at one or more such sites and a fluorophore coupled thereto so that fluorescence intensity of the fluorophore changes upon ligand binding.

bPBPs suitable for use in the present method can be selected or designed. The bPBP superfamily is well suited for the redesign of ligand-binding specificities either by computational methods or by other means or both based on the ligand to be detected (see, for example, analytes referenced in Table 1). Sites on the bPBP appropriate for attachment of one or more reporters (e.g., fluorophores or redox cofactors) include allosteric sites, peristeric sites, and endosteric sites (a reporter can also be present at a non-signaling site for use, for example, as a reference). In the case of an allosteric site, the reporter (e.g., fluorophore) can be placed at one or more locations distant from the ligand-binding site (i.e., distal from the ligand-binding pocket) that undergo local conformational changes upon ligand binding. In the case of a peristeric site, the reporter (e.g., fluorophore) can be positioned on the "rim" of the binding site but not such that it directly interacts with the ligand. With an endosteric site, the reporter (e.g., fluorophore) can be present in the binding site so that it interacts directly with the ligand. The latter two examples show attachment proximal to the ligand-binding pocket.

Table 1. Potential applications of biosensors for bPBP ligands

	application		
analyte	clinical	industrial	environmental
arabinose		Deanda et al., 1996	
glucose	Burrin & Price, 1985	AOAC, 1995	
maltose	Nelson et al., 1977	AOAC, 1995	
ribose		AOAC, 1995	
glutamate	Burtis & Ashwood, 1994	AOAC, 1995	
glutamine	Smith and Forman, 1994		
histidine	Taylor et al., 1991		
dipeptides			
phosphate	Burkhardt et al., 1979		APHA, 1992
sulfate			EPA, 1999
Fe(III)			Martin, 1992

Allosteric, peristeric, and endosteric sites can be designed in at least two different ways, as detailed in the Example that follows. Generally, a structure-based design approach can be used in which the structures of the open and closed states (for allosteric designs) or the closed state only (for peristeric and endosteric designs) are examined. Alternatively, a sequence-based design approach can be used wherein homology relationships can be exploited to predict the location of cysteine mutations in proteins the three-dimensional structures of which have not been determined, provided that such mutations have been characterized in proteins of known structure.

As indicated above, reporters suitable for use in the invention include, but are not limited to, fluorophores and redox cofactors. In the case of fluorophores, the choice is dependent, at least in part, on the nature of the location within the particular protein. While one fluorophore may function better in a certain location than another, one skilled in the art can readily select the preferred fluorophore for a particular application (see, for

example, U.S. Patent 6,277,627). In the Example that follows, eight different fluorophores are used in the design of fluorescent sensors for:

Arabinose	Arabinose binding protein (ABP)
Dipeptides	Dipeptide binding protein (DPP)
Glutamate and asparate	Glu/Asp binding protein (EBP)
Glutamine	Glutamine binding protein (QBP)
Fe(III)	Iron binding protein (FeBP)
Histidine	Histidine binding protein (HBP)
Maltose	Maltose binding protein (MBP)
Glucose	Glucose binding protein (GBP)
Phosphate	Phosphate binding protein (PhBP)
Sulfate	Sulfate binding protein (SBP).

The invention, however, is in no way limited to these specific embodiments.

Redox reporters for use in the invention can be a redox-active metal center or a redox-active organic molecule. It can be a natural organic cofactor such as NAD, NADP, FAD or a natural metal center such as Blue Copper, iron-sulfur clusters, or heme, or a synthetic center such as an organometallic compound such as a ruthenium complex, organic ligand such as a quinone, or an engineered metal center introduced into the protein or engineered organic cofactor binding site. Cofactor-binding sites can be engineered using rational design or directed evolution techniques. The redox reporter can be covalently or non-covalently attached to the protein, either by site-specific or adventitious interactions between the cofactor and protein. It can be intrinsic to the protein such as a metal center (natural or engineered) or natural organic (NAD, NADP, FAD) or organometallic cofactor (heme), or extrinsic (such as a covalently conjugated, synthetic organometallic cluster). The redox reporter can be, for example, bound (e.g., covalently) at a position where the amino acid residue is on the protein's surface.

The redox reporter can be a metal-containing group (e.g., a transition metal-containing group) that is capable of reversibly or semi-reversibly transferring one or more electrons. A number of possible transition metal-containing reporter groups can be used.

Advantageously, the reporter group has a redox potential in the potential window below that subject to interference by molecular oxygen and has a functional group suitable for covalent conjugation to the protein (e.g., thiol-reactive functionalities such as maleimides or iodoacetamide for coupling to unique cysteine residues in the protein). The metal of the reporter group should be substitutionally inert in either reduced or oxidized state (i.e., advantageously, exogenous groups do not form adventitious bonds with the reporter group). The reporter group can be capable of undergoing an amperometric or potentiometric change in response to ligand binding. In a preferred embodiment, the reporter group is water soluble, is capable of site-specific coupling to a protein (e.g., via a thiol-reactive functional group on the reporter group that reacts with a unique cysteine in the protein), and undergoes a potentiometric response upon ligand binding. Suitable transition metals for use in the invention include, but are not limited to, copper (Cu), cobalt (Co), palladium (Pd), iron (Fe), ruthenium (Ru), rhodium (Rh), osmium (Os), rhenium (Re), platinum (Pt), scandium (Sc), titanium (Ti), vanadium (V), chromium (Cr), manganese (Mn), nickel (Ni), molybdenum (Mo), technetium (Tc), tungsten (W), and iridium (Ir). That is, the first series of transition metals, the platinum metals (Ru, Rh, Pd, Os, Ir, and Pt), along with Fe, Re, W, Mo, and Tc, are preferred. Particularly preferred are metals that do not change the number of coordination sites upon a change in oxidation state, including ruthenium, osmium, iron, platinum and palladium, with ruthenium being especially preferred.

The reporter group can be present in the biosensor as a covalent conjugate with the protein or it can be a metal center that forms part of the protein matrix (for instance, a redox center such as iron-sulfur clusters, heme, Blue copper, the electrochemical properties of which are sensitive to its local environment). Alternatively, the reporter group can be present as a fusion between the protein and a metal binding domain (for instance, a small redox-active protein such as a cytochrome). Preferably, the reporter group is covalently conjugated to the protein via a maleimide functional group bound to a cysteine (thiol) on the protein. In any case, the reporter group is attached to the protein so that it is located between the protein and the electrode.

Engineered proteins of the invention can be produced by site-specifically introducing a reporter group(s) by total synthesis, semi-synthesis, or gene fusions (see, for example, Adams et al., Nature 39:694-697, 1991; Brune et al., Biochemistry 33:8262-

8271, 1994; Gilardi et al., Anal. Chem. 66:3840-3847, 1994; Godwin et al., J. Am. Chem. Soc. 118:6514-6515, 1996; Marvin et al., Proc. Natl. Acad. Sci. U.S.A. 94:4366-4371, 1997; Post et al., J. Biol. Chem. 269:12880-12887, 1994; Romoser, J. Biol. Chem. 272:13270-13274, 1997; Thompson et al., J. Biomed. Op. 1:131-137, 1996; Walkup et al., J. Am. Chem. Soc. 119:5445-5450, 1997).

Assays for ligand may be performed with the biosensor. A sample is contacted with the biosensor under appropriate assay conditions. Ligand present in the sample, if any, may be detected by binding to the biosensor and measuring the signal transduced by ligand-bound biosensor in the assay. For detection purposes, binding does not need to be quantitative because a simple determination of whether the ligand is present or absent (within detection limits) needs to be performed. Otherwise, comparison to a series of control samples (e.g., known quantities of ligand) may be required to quantitate the amount or concentration of ligand in the sample. Given the volume of the sample, the amount (i.e., mass) of ligand and the concentration of ligand are interconvertible. A blank sample containing no ligand may be used to determine background signal. Standards may be used to construct a standard curve (e.g., hyperbolic) used to quantitate unknown samples. Although homogeneous assay formats (i.e., those requiring no separation of bound and non-bound ligand) are preferred, separation in a heterogeneous assay format may be required if substances which significantly interfere with signal transduction and/or measurement are present in the sample. Signal transduction preferably does not require the addition of exotic reagents so assays of body fluids may be performed with minimal sample preparation and under physiological conditions. They may even be performed *in vivo* if the biosensor is adapted to an implantable medical device. Alternatively, a biosensor in contact with the skin may assay interstitial fluid or perspiration. Lavage may be used to sample mucosal tissues.

The sample can be obtained in a laboratory setting (e.g., clinic or research institution); from an environmental source (e.g., air, aquafers and other bodies of water, animal or plant products grown on the land, soil); from an industrial source (e.g., the food, biopharmaceutical, chemical, or other manufacturing industries). The analyte to be assayed is identical to the ligand, comprised of multiple copies of the ligand, chemically related to the ligand such that it is identified by a change in signal transduction (e.g., a related chemical structure is more strongly or more weakly bound by the biosensor as

compared to its "correct" ligand), or any combination thereof. The change in signal transduction may be correlated to the change in chemical structure such that the non-identical analyte is identified (see below description of integrative assays). Examples of ligands which may be detected or quantitated include: amino acids; carbohydrates; bioactive solid and gaseous compounds which are soluble in an aqueous sample; contraband or controlled substances (i.e., substances which are illegal to use or possess, or which are highly regulated); environmental pollutants (e.g., phosphates, sulfates); explosives (e.g., TNT); food contaminants and byproducts (e.g., carcinogens, plant toxins, teratogens); lipids; metal ions (e.g., divalent cations, ferric ions); microbial toxins (e.g., toxic products of viruses, bacteria, or protozoa); neurotransmitters (e.g., serotonin); nucleosides or nucleotides (e.g., NAD, NADP, FAD); peptides or steroids (e.g., growth factors, hormones, morphogenic or developmental signals); and therapeutic drugs. Objects (e.g., baggage, mail, other containers); people or vehicles passing through a checkpoint; and borders or secure areas may be inspected for biological agents, contraband, explosives, poisons, and toxins in security or military applications.

One or more biosensors may be covalently or noncovalently attached to a solid or porous substrate. The substrate may be flat and planar (e.g., filter membrane, glass slide, semiconductor chip); cylindrical (e.g., optical fiber, plastic rod); spherical (e.g., crosslinked polymer or glass bead); or formed as a container (e.g., cell or cuvette, multiwell plate). The substrate may be fabricated for analysis by instruments which measure the signal transduced by the reporter group (e.g., microscope, photometer, spectrometer). Individual biosensors may be coded by an attached marker (e.g., bar code, radio frequency or RFID, or biopolymer) which can be decoded by a reader (e.g., scanner of light-and-dark patterns, radio receiver, specific binding probe or automated sequencer) or separated by a sorter in accordance with their marker. The code identifying each biosensor may be used in parallel analysis by rapidly assaying a sample for a plurality of ligands. Multiple biosensors with different ligand-binding specificities are used in the same assay to detect and/or quantitate multiple ligands at the same time. Alternatively, attaching different biosensors at particular spots on the substrate may be used to identify their ligand-binding specificities by where the signals are being produced. Signals may be authenticated by repeating the assay, using multiple biosensors with the same specificity for redundant assays, or correlating the results from multiple biosensors with overlapping specificities for integrative assays. In the latter, particular reactivity patterns of the

biosensors are correlated with the identity of the analyte bound by them. Analytes that are more closely related in their chemical structure to the ligand will bind more strongly to the cognate biosensor. Signals from a plurality of biosensors with overlapping, known ligand-binding specificities are integrated to deduce the identity of the analyte.

The invention relates, in further embodiments, to biosensors constructed using the above-described methods and to the use thereof in analyte detection in, for example, clinical, industrial, and environmental settings. Particular utilities are described in the specific Example that follows. Provided is a description of a number of sites that can be used for optical glucose sensors based on GBP (W183C conjugated to acrylodan has been used successfully in fiber-optic prototypes of a glucose sensor).

To the extent that specific biosensors constructed in accordance with the present approach may be present in the public domain (e.g., may be disclosed in Marvin et al., Proc. Natl. Acad. Sci. USA 94:4366-4371, 1997 or in U.S. Patent 6,277,627), such biosensors are not within the scope of the present invention.

Certain aspects of the invention can be described in greater detail in the non-limiting Example that follows.

EXAMPLE

Experimental Details

Molecular Cloning. PCR was used to amplify wild-type genes for bPBPs from genomic DNA of *E. coli* strain CSH100 (arabinose, dipeptide, histidine, ribose, sulfate, and glutamate/aspartate BP); strain W1485 (glucose and glutamine BP) and strain RU1012 (phosphate BP), or of *H. influenzae* strain Rd (Fe(III) BP). Amplified products were cloned into one of the protein expression vectors pAED4 (Doering, "Functional and structural studies of a small f-actin binding domain" in Ph.D. thesis, Massachusetts Institute of Technology, 1992); pKK223-3 (Brosius & Holy, Proc. Natl. Acad. Sci. USA 81:6929-6933, 1984); or pET vectors (Studier et al., Meth. Enzymol. 185:60-89, 1990) (Novagen). N-terminal oligonucleotide primers were designed to clone only the processed periplasmic form, deleting the signal sequence. The C-terminal primer was designed to append the sequence Gly-Ser-Gly-$(His)_n$ or Gly-Ser-$(His)_n$, where n=5, 6, or 10. Two

tandem stop codons (TAATGA) follow the last His codon. Maltose BP mutants were made in and expressed from plasmid pMAL-c2X (New England BioLabs). *E. coli* strains XL1-BLUE (Stratagene) and DH5α (Hanahan, J. Mol. Biol. 166:557-580, 1983) were used for plasmid construction. Single amino acid substitutions were generated by overlapping PCR mutagenesis (Ho et al., Gene 77:51-59, 1989). All clones and mutations were confirmed by nucleotide sequencing. In the case of arabinose BP, the single cysteine in the wild type sequence was replaced by alanine to eliminate the possibility of reporter group conjugation to this thiol (Miller et al., J. Biol. Chem. 254:7521-7528, 1979). Additionally the sequence of Fe(III) BP was mutated by substitution of Glu57 with Asp to raise the K_d to a concentration range conveniently measured using Fe(III) citrate.

Protein Expression. Plasmids were transformed into *E. coli* strain BL21-DE3, grown in nutrient broth overnight at 37°C, then diluted 100-fold into fresh medium and grown further at 37°C or 25°C. Expression was induced by the addition of isopropyl β-D-1-thiogalactopyranoside to 1 mM when the optical density of the culture at 600 nm reached 0.4. After 2 to 4 hours, cells were harvested by centrifugation, resuspended in 20 mM 3-morpholinopropanesulfonic acid (MOPS), 100 mM NaCl, pH 6.9 and stored frozen or lysed immediately for protein purification.

Protein Purification. Cells were lysed by sonication or by passage through a French pressure cell. The lysate was treated by adding Polymin P to 0.33% (w/v), chilling on ice for 15 min, then centrifuging to pellet cell debris. The supernatant was loaded on a Ni(II)-charged column of Chelating Sepharose™ Fast Flow (Amersham Pharmacia Biotech) equilibrated with 20 mM MOPS, 500 mM NaCl, 10 mM imidazole, pH 7.5. The column was washed with loading buffer, then with the same containing 60 mM imidazole, followed by the same with 100 mM imidazole. Finally, protein was eluted with loading buffer containing 400 mM imidazole, and was collected in fractions and assessed for purity by gel electrophoresis. All preparations were at least 95% pure by this criterion. Protein-containing fractions were dialyzed exhaustively against buffer (20 mM MOPS, 100 mM NaCl, pH 6.9, or 20 mM NaH_2PO_4, 100 mM NaCl, pH 6.9) or desalted by gel filtration to remove bound ligand.

Fluorophore conjugation to cysteine-substituted bPBPs. Thiol-reactive fluorophores obtained from Molecular Probes (Eugene, Oregon) were 5-iodoacetamidofluorescein (fluorescein); N-(1-pyrene) iodoacetamide (pyrene); N,N'-

dimethyl-N-(iodoacetyl)-N'-(7-nitrobenz-2-oxa-1,3-diazol-4-yl)ethylenediamide (NBD); N-((2-(iodoacetoxy)ethyl)-N-methyl)amino-7-nitrobenz-2-oxa-1,3-diazole (NBDE); and 6-acryloyl-2-dimethylaminonaphthalene (acrylodan). The styryl and naphthyl dyes JPW4039, JPW4042, and JPW4045 (Fig. 3) were synthesized at the University of Connecticut. All fluorophore conjugation steps were typically carried out at room temperature. To protein at a concentration of 100 μM was added tris-(2-carboxyethyl)phosphine HCl to a five-fold molar excess to reduce intermolecular disulfide bonds. A thiol-reactive fluorophore (20 to 25 mM in acetonitrile or dimethyl sulfoxide) was added in small aliquots to a five-fold molar excess over protein. Conjugation proceeded in the dark at room temperature for 4 hours, or overnight at 4°C. Separation of protein from unreacted fluorophore was achieved by exhaustive dialysis or by size-exclusion chromatography. The efficiency of reporter group attachment was assessed by determination of unreacted thiol with Ellman's reagent (Ellman, Arch. Biochem. Biophys. 74:443-450, 1958) or by measuring the ratio of fluorophore to protein from absorbance spectra of the purified conjugate.

Depletion of sulfate and phosphate. Solutions of sulfate BP and phosphate BP and their buffers were treated to decrease the concentration of contaminating sulfate and phosphate, respectively. Sulfate BP buffer (20 mM Tris-HCl, pH 8.0) was passed through the chloride form of Dowex 1X2-100 strongly basic anion-exchange resin. Sulfate BP solutions were treated by dialysis against treated buffer; Dowex resin held in a separate dialysis tube was also included. Phosphate BP solutions and buffer (20 mM MOPS, 100 mM NaCl, pH 6.9) were depleted of phosphate by addition of 7-methylguanosine to 1 mM and dialyzed against bacterial nucleoside phosphorylase (1 unit ml^{-1}) (Sigma-Aldrich) partitioned in a separate dialysis tube (Brune et al., Biochem. 33:8262-8271, 1994).

Fluorimetry. All measurements were conducted with an SLM Aminco-Bowman series 2 fluorimeter, with sample stirring at 25°C. Fluorescence emission spectra were acquired with excitation and emission slit widths of 4 and 8 nm, respectively. Photomultiplier tube potential was maintained between 400 and 800 volts. Protein concentrations were in the range of 50 to 1000 nM. Fluorophore-specific excitation was at the following approximate wavelengths: tryptophan, 290 nm; acrylodan, 390 nm; fluorescein, 485 nm; pyrene, 340 nm; NBD and NBDE, 490 nm; JPW4039, 485 nm; JPW4042, 470 nm; JPW4045, 470 nm.

To measure ligand binding affinity, ligand was serially added to 3 ml of bPBP at a concentration of 50 to 1000 nM, and emission intensities recorded. Corrections were made for dilution of the protein and for background signal from buffer. Binding curves were fit to binding isotherms using equation 3 or 4, as appropriate.

Fe(III) BP has a dissociation constant for Fe(III) on the order of 10^{-21} M (Adhikari et al., J. Biol. Chem. 270:25142-25149, 1995), hindering accurate fluorescence-based measurements of affinity at nanomolar protein concentrations. Hence we used Fe(III) citrate (logK ~ 10.25) (Martell and Smith, *Critical Stability Constants*, Plenum Press, New York, 1977) as the ligand in a competition assay.

Results

Family of biosensors. A set of eleven bPBPs with widely varying ligand-binding specificities was selected for engineering biosensor function (Table 2). All were from *E. coli* except Fe(III) BP, which is from *Haemophilus influenzae*. Binding specificities and affinities of these proteins for their respective ligands have been characterized (references in Table 2). Three proteins bind monosaccharides (arabinose, glucose and ribose BP), one binds di- and trisaccharides of glucose (maltose BP), three bind amino acids (glutamate/aspartate, histidine, and glutamine BP), one binds di- and tripeptides (dipeptide BP), two bind oxyanions (phosphate and sulfate BP), and one binds a metal ion (Fe(III) BP). Most of these bPBPs bind at most two or three related ligands with high affinity (micromolar or better). For example, phosphate BP binds phosphate and arsenate but not other oxyanions (Luecke & Quiocho, Nature 347:402-406, 1990), while glucose BP binds glucose and galactose but not other monosaccharides (Anraku, J. Biol. Chem. 243:3116-3122, 1968). Dipeptide BP is an exception in that it binds a wide variety of di- and tripeptides (Smith et al., Microbiology 145:2891-2901, 1999). Measured ligand dissociation constants in these proteins are typically in the range of 0.1 to 1 μM. An exception is Fe(III) BP, where the K_d for $Fe(III)_{(aq)}$ is estimated to be 10^{-21} M in competition assays with Fe(III) chelates (Adhikari et al., J. Biol. Chem. 270:25142-25149, 1995).

Table 2. References and PDB[a] files for bPBP structures, genes, and ligand binding

	crystal structure		DNA sequence	ligand affinity
bPBP	open form	closed form		
arabinose BP		Quiocho and Vyas, 1984 1ABE	Scripture et al., 1987	Clark et al., 1982; Miller et al., 1983
dipeptide BP	Nickitenko et al., 1995 1DPE	Dunten & Mowbray, 1995 1DPP	Abouhamad et al., 1991	Guyer et al., 1986; Smith et al., 1999
Glu/Asp BP				Barash Halpern, 1975; Willis Furlong, 1975
Fe(III) BP	Bruns et al., 2001 1D9V	Bruns et al., 1997 1MRP	Sanders et al., 1994	Adhikari et al., 1995
glucose BP		Vyas et al., 1988; Vyas et al., 1994 1GLG	Scholle et al., 1987	Anraku, 1968
histidine BP		Yao et al., 1994 1HSL	Joshi & Ames 1996	Miller et al., 1983
maltose BP	Sharff et al., 1992 1OMP	Spurlino et al., 1991; Quiocho et al., 1997 1ANF	Duplay et al., 1984	Schwartz et al., 1976
phosphate BP	Ledvina et al., 1996 1OIB	Luecke & Quiocho, 1990 1IXH	Magota et al., 1984	Medveczky & Rosenberg, 1969
glutamine BP	Hsiao et al., 1996 1GGG	Sun et al., 1998 1WDN	Nohno et al., 1986	Weiner et al., 1971
ribose BP	Bjorkman & Mowbray, 1998 1URP	Mowbray & Cole, 1992 2DRI	Groarke et al., 1983	Willis & Furlong, 1974
sulfate BP		Pflugrath & Quiocho, 1985; He & Quiocho, 1993 1SBP	Hellinga & Evans, 1985	Jacobson & Quiocho, 1988

a: Protein Data Bank (Berman et al., 2000)

Abouhamad et al., Molec. Microbiol. 5:1035-1047 (1991)
Adhikari et al., J. Biol. Chem. 270:25142-25149 (1995)
Anraku, J. Biol. Chem. 243:3116-3122 (1968)
Barash & Halpern, Biochim. Biophys. Acta 386:168-180 (1975)
Bjorkman & Mowbray, J. Mol. Biol. 279:651-664 (1998)
Bruns et al., Biochemistry 40:15631-15637 (2001)
Bruns et al., Nat. Struct. Biol. 4:919-924 (1997)
Clark et al., Biochemistry 21:2227-2233 (1982)
Dunten & Mowbray, Protein Sci. 4:2327-2334 (1995)
Duplay et al., J. Biol. Chem. 259:10606-10613 (1984)
Groarke et al., J. Biol. Chem. 258:12952-12956 (1983)
Guyer et al., J. Bacteriol. 168:775-779 (1986)
He & Quiocho, Protein Sci. 2:1643-1647 (1993)
Hellinga & Evans, Eur. J. Biochem. 149:363-373 (1985)
Hsiao et al., J. Mol. Biol. 262:225-242 (1996)
Jacobson & Quiocho, J. Mol. Biol. 204:783-787 (1988)
Joshi & Ames, GenBank Accession Number U47027 (1996)
Ledvina et al., Proc. Natl. Acad. Sci. USA 93:6786-6791 (1996)
Luecke & Quiocho, Nature 347:402-406 (1990)
Magota et al., J. Bacteriol. 157:909-917 (1984)
Medveczky & Rosenberg, Biochim. Biophys. Acta 192:369-371 (1969)
Miller et al., J. Biol. Chem. 258:13665-13672 (1983)
Mowbray & Cole, J. Mol. Biol. 225:155-175 (1992)
Nickitenko et al., Biochemistry 34:16585-16595 (1995)
Nohno et al., Molec. Gen. Genet. 205:260-269 (1986)
Pflugrath & Quiocho, Nature 314:257-260 (1985)
Quiocho et al., Structure 5:997-1015 (1997)
Quiocho & Vyas, Nature 310:381-386 (1984)
Sanders et al., Infect. Immun. 62:4515-4525 (1994)
Scholle et al., Molec. Gen. Genet. 208:247-253 (1987)
Scripture et al., J. Mol. Biol. 197:37-46 (1987)
Schwartz et al., Eur. J. Biochem. 71:167-170 (1976)
Sharff et al., Biochemistry 31:10657-10663 (1992)
Smith et al., Microbiology 145:2891-2901 (1999)
Spurlino et al., J. Biol. Chem. 266:5202-5219 (1991)
Sun et al., J. Mol. Biol. 278:219-229 (1998)
Vyas et al., Biochemistry 33:4762-4768 (1994)
Vyas et al., Science 242:1290-1295 (1988)
Weiner et al., Arch. Biochem. Biophys. 142:715-717 (1971)
Willis & Furlong, J. Biol. Chem. 249:6926-6929 (1974)
Willis & Furlong, J. Biol. Chem. 250:2574-2580 (1975)
Yao et al., Biochemistry 33:4769-4779 (1994)

For nine of the eleven proteins selected for this study crystal structures have been solved of the closed, ligand-bound state (Table 2). In the case of sulfate BP, the crystal

structure of the *E. coli* protein has not been reported, so that of *Salmonella typhimurium* sulfate BP was adopted to model the *E. coli* protein. Sulfate BP from *E. coli* and *S. typhimurium* are 95% identical in amino acid sequence and hence likely to have highly similar structures, in analogy to histidine BP from these two organisms (Oh et al., J. Biol. Chem. 269:4135-4143, 1994; Yao et al., Biochemistry 33:4769-4779, 1994). Structures have been solved for the open unliganded state for six of the eleven proteins as well (Table 2).

Structure-based design of conformational coupling. Coupling between ligand binding and a change in the fluorescent signal of a covalently attached, environmentally sensitive fluorophore can be established if the local environment of the fluorophore changes as a result of formation of the complex and a linked conformational change. Two mechanisms can be distinguished to establish such structural linkage relationships. Direct linkage involves formation of a non-bonded contact between the bound ligand and the conjugated fluorophore. Indirect linkage involves changes in the local protein structure in the immediate vicinity of the attached fluorophore, and relies on ligand-mediated conformational changes such as the hinge-bending motion observed in the bPBPs.

Direct linkage relationships are readily designed by replacing a residue known to form a ligand contact with a cysteine to which the fluorophore is attached ("endosteric" attachment site). Indirect linkage relationships can be established in two ways. The most straightforward method relies on visual inspection of the ligand complex structure, and identifying residues that are located in the vicinity of the binding site, but do not interact directly with the ligand, and that are likely to be involved in conformational changes. In the case of the bPBPs, such are residues located at the perimeter of the inter-domain cleft that forms the ligand binding site. The environment of these "peristeric" sites changes significantly upon formation of the closed state. These are examples of positions which are proximal to the ligand-binding pocket. The second approach identifies sites in the protein structure that are located some distance away from the ligand-binding site (i.e., distal to the ligand-binding pocket), and undergo a local conformational change in concert with ligand binding. If the structures of both the open and closed states are known, then such "allosteric" sites can be identified using a computational method that analyzes the conformational change (Marvin et al., Proc. Natl. Acad. Sci. USA 94:4366-4371, 1997). Alternatively, once allosteric sites have been identified in one bPBP, modeling and

structural homology arguments can be invoked to identify such sites in other bPBPs in which only one state has been characterized (Marvin & Hellinga, J. Am. Chem. Soc. 120:7-11, 1998). Table 3 summarizes the designs of all three classes of sites in each of the receptors used in this study. The locations of these sites in the eleven bPBPs are shown in Figure 1.

Table 3. Fluorophore conjugation sites

protein	mutant	steric category[a]	design method[b]	protein	mutant	steric category[a]	design method[b]
arabinose BP	D257C	a	3	histidine BP	E167C	p	1
	F23C	a	3		K229C	p	1
	K301C	a	3		V163C	p	1
	L253C	a	3		Y230C	p	1
	L298C	a	3		F231C	p	1
dipeptide BP	D450C	p	1		Y88C	a	3
	K394C	p	1	maltose BP	D95C	a	2
	R141C	p	1		F92C	a	2
	S111C	p	1		I329C	a	2
	T44C	p	1		S233C	p	2
	W315C	p	1	phosphate BP	A225C	a	2
Glu/Asp BP	A207C	p	4		N223C	a	2
	A210C	p	4		N226C	a	2
	E119C	p	4		S164C	p	2
	F126C	a	4		S39C	p	2
	F131C	a	4	glutamine BP	N160C	p	2
	F270C	p	4		F221C	p	2
	G211C	p	4		K219C	p	2
	K268C	p	4		L162C	p	2
	Q123C	p	4		W220	p	2
	T129C	a	4		Y163C	p	2
Fe(III) BP	E203C	p	1		Y86C	a	2
	K202C	p	1	ribose BP	T135C	p	2
	K85C	a	1		D165C	p	2
	V287C	a	1		E192C	p	2
glucose BP	Y10C	e	1		A234C	a	2
	N15C	p	1		L236C	a	2
	E93C	p	1		L265C	a	2
	E149C	p	1	sulfate BP	L65C	p	1
	H152C	e	1		N70C	p	1
	W183C	e	1		Q294C	p	1
	L255C	a	3		R134C	p	1
	D257C	a	3		W290C	p	1
	V296C	a	3		Y67C	p	1

a: a, allosteric; e, endosteric; p, peristeric

b: 1, visual inspection of the closed structure; 2, identification by automated comparison of the open and closed states; 3, structural homology; 4, sequence homology

Sequence-based design of conformational coupling. The number of bPBPs of known sequence greatly exceeds the number for which structures have been solved or for

which functions have been assigned by genetic or biochemical characterization. To exploit this reservoir of potential biosensors, coding sequences for bPBPs must be identified and their putative ligand-binding specificities must be established. The identification of bPBPs in microbial genomes relies on finding amino acid sequence homologies to particular clusters of the bPBP family (Tam & Saier, Microbiol. Rev. 57:320-346, 1993). Ligand-binding can then be determined by direct experimentation, or be inferred either by structural relationships to bPBPs of known function, or by establishing genetic linkage to other genes of known function (Pellegrini et al., Proc. Natl. Acad. Sci. USA 96:4285-4288, 1999). Subsequently sites within the homolog that undergo local conformational change, and to which reporter functions can be attached, must be identified. The selection of sites for attaching reporter functions relies on homology to bPBPs of known structure.

To illustrate these principles, a glutamate biosensor was constructed starting from genome sequence data only. The genome of *E. coli* K12 contains the locus *ybeJ* encoding a protein identified as a putative bPBP based on amino acid sequence homology with glutamine and histidine BPs (26% and 23% sequence identity; 41% and 43% sequence similarity, respectively) (Blattner et al., Science 277:1453-1474, 1997). The assignment of YBEJ as an amino-acid binding protein was strengthened by the presence of conserved residues found to be associated with binding to the α-amino and α-carboxylate groups of the ligand in all bPBP amino-acid binding proteins of known structure identified in *E. coli* (Table 4). Of additional interest is the presence of an arginine residue in YBEJ located at a position that in the other amino acid-binding proteins interacts directly with the side chain of the bound amino acid, suggesting that YBEJ binds an amino acid bearing a negatively charged side chain. Finally, *ybeJ* is located adjacent to three tandem genes (*gltJ*, *gltK*, *gltL*) postulated to be involved in the glutamate/aspartate transport system (Lum & Wallace, GenBank Accession Number U10981, 1995), suggesting that *ybeJ* encodes a glutamate/aspartate BP. Putative allosteric, endosteric, and peristeric sites were identified from a structure-based sequence alignment of YBEJ with glutamine BP and histidine BP (Figure 2).

Table 4. Ligand interactions with residues in polar amino-acid binding proteins

ligand group*	sc	sc	sc	αN	αN	αC	sc	sc	αC	αN
glutamine BP	D10	F13	F50	G68	T70	R75	K115	T118	G119	D157
histidine BP	D11	Y14	L52	S70	S72	R77	L117	T120	T121	D161
lys/arg/orn BP	D11	Y14	F52	S70	S72	R77	L117	T120	T121	D161
YBEJ	R25	S28	S73	S91	T93	R98	T137	T140	T141	D183

* sc: side chain, αN: α-amino, αC: α-carboxy

Mutagenesis and protein production All the genes for the bPBPs used in this study were cloned from *E. coli* or *H. influenzae* genomic DNA using PCR. The leader peptide sequence that directs expression into the periplasm was identified by comparison to the known N-terminus of the protein, or, in the case of YBEJ, by homology to known leader sequences (von Heijne, Nucl. Acids Res. 14:4683-4690, 1986). The protein was produced by over-expression of the processed form in the cytoplasm with an initiation methionine placed just before the N-terminus of the processed protein, under the control of a strong inducible promoter in the pAED4 (Doering, "Functional and structural studies of a small f-actin binding domain" in Ph.D. thesis, Massachusetts Institute of Technology, 1992); pET-21a (Studier et al., Meth. Enzymol. 185:60-89, 1990) (Novagen); or pKK223-3 (Blattner et al., Science 277:1453-1474, 1997) plasmids. An oligohistidine tag was fused to the carboxy terminus of the cloned receptor to permit facile purification by immobilized metal affinity chromatography (Hochuli et al., J. Chromatogr. A 411:177-184, 1987). In all cases, the receptors expressed well (at least 50 mg of pure protein per liter of fermentation). The molecular masses estimated by gel electrophoresis corresponded to the predicted mass of the expressed reading frame.

Cysteine point mutations were introduced by the PCR overlap method (Ho et al., Gene 77:51-59, 1989). Mutant proteins typically expressed as well as the wild type protein. All cysteine substitutions in arabinose BP were constructed in the C64A background to prevent interference from this endogenous cysteine (Miller et al., J. Biol. Chem. 254:7521-7528, 1979). In the case of Fe(III) BP, all mutations were constructed in

the E57D background. In the crystal structure of Fe(III) BP, this glutamate is coordinated to the iron (Bruns et al., Nat. Struct. Biol. 4:919-924, 1997). It was found that the E57D mutation weakens the affinity of Fe(III) BP for Fe(III) from approximately $1x10^{-21}$ (Adhikari et al., J. Biol. Chem. 270:25142-25149, 1995) to approximately $3x10^{-8}$, assuming a stability constant for the 1:1 Fe(III) citrate complex of logK=10.25 (Martell & Smith, *Critical Stability Constants*, Plenum Press, New York, 1977). This permitted straightforward determination of Fe(III) affinity by direct titration with Fe(III) citrate at nanomolar concentrations of Fe(III) BP.

Signal transduction by fluorescence. To report ligand binding by the set of eleven bPBPs, fluorescent reporter groups were attached to single cysteine thiols engineered into sites that were predicted to undergo binding-dependent conformational change. Eight thiol-reactive fluorophores were examined that were chosen on the basis of the sensitivity of their emission spectra to changes in environment and spanning a wide range of emission and excitation wavelengths (Fig. 3). The results for biosensor conjugates which are illustrative of the invention are presented in Table 5 (11 receptors, 68 cysteine mutants, 320 fluorophore conjugates).

Table 5. Spectral and binding parameters of fluorophore-conjugated bPBPs

protein[a]	mutant	site[b]	fluorophore	ligand	$\lambda_{max,\ apo}$	$\lambda_{max,\ sat}$	ΔI_{std} [c]	inc/dec[d]	ΔR_{max} [c]	K_d (μM)	std error
arabinose BP	D257C	a	JPW4039	arabinose	600	596	**0.38**	-	0.92	90	3
			Acrylodan		495	495	**0.26**	-	**1.66**	56	7
			Fluorescein		519	520	0.03	-	1.17	4.0	0.4
			NBD		538	544	0.22	+	1.15	32	2
	F23C	a	JPW4039		587	588	**0.93**	-	0.76	38	1
			Acrylodan		503	503	0.02	+	0.99	3.9	0.6
			Fluorescein		519	519	0.04	-	0.45	3.2	0.5
			NBD		543	548	**0.38**	-	0.76	5.0	0.1
	K301C	a	JPW4039		582	588	**1.20**	-	**1.73**	77	4
			Acrylodan		486	486	0.10	-	1.19	0.46	0.01
			Fluorescein		518	517	**0.41**	+	1.06	24	1
			NBD		532	538	0.08	-	**3.15**	31	1
	L253C	a	JPW4039		590	589	**0.83**	-	**1.31**	165	8
			Acrylodan		482	495	0.05	-	**1.81**	0.69	0.10
			Fluorescein		519	515	0.24	-	**2.71**	48	3
			NBD		539	539	**0.41**	+	1.66	775	49

Table 5. Spectral and binding parameters of fluorophore-conjugated bPBPs

protein[a]	mutant	site[b]	fluorophore	ligand	$\lambda_{max,\ apo}$	$\lambda_{max,\ sat}$	ΔI_{std} [c]	inc/dec[d]	ΔR_{max} [c]	K_d (μM)	std error
	L298C	a	JPW4039		591	591	**0.42**	-	0.65	70	2
			Acrylodan		499	500	0.07	-	**1.77**	44	2
			Fluorescein		518	518	0.02	-	0.48		
			NBD		543	539	**0.45**	+	0.41	56	4
dipeptide BP	D450C	p	JPW4039	Gly-Leu	602	604	0.20	-	0.29	0.91	0.20
			JPW4042		666	664	0.20	-	1.08	1.5	0.3
			JPW4045		663	666	0.23	-	1.18	2.0	0.5
			Acrylodan		508	521	0.06	+	**1.64**	11	4
			Fluorescein		520	520	0.10	+	0.04		
			NBD		545	544	0.02	-	0.80		
	K394C	p	JPW4039		592	598	**0.37**	+	**1.34**	30	2
			JPW4042		638	644	0.06	+	0.99	78	8
			JPW4045		631	640	0.01	+	1.07		
			Acrylodan		500	500	0.23	+	0.90	23	2
			Fluorescein		522	522	**0.30**	+	0.21	93	6
			NBD		542	541	0.06	-	0.68	0.012	0.005

Table 5. Spectral and binding parameters of fluorophore-conjugated bPBPs

protein[a]	mutant	site[b]	fluorophore	ligand	$\lambda_{max,\ apo}$	$\lambda_{max,\ sat}$	ΔI_{std} [c]	inc/dec[d]	ΔR_{max} [c]	K_d (μM)	std error
	R141C	p	JPW4039		592	596	0.06	-	0.69		
			JPW4042		629	631	0.06	-	0.87		
			JPW4045		610	617	0.15	-	1.18		
			Acrylodan		502	501	0.06	-	0.25	2.3	1.2
			Fluorescein		522	522	0.12	-	0.66	38	14
			NBD		542	544	0.00	+	0.13		
	S111C	p	JPW4039		597	598	0.24	+	0.33	34	14
			JPW4042		644	644	0.18	+	1.49	15.8	1.5
			JPW4045		634	642	0.01	-	1.07		
			Acrylodan		499	501	0.11	+	1.61	4.8	2.3
			Fluorescein		521	521	0.07	-	0.18	2.6	1.9
			NBD		538	542	0.01	+	0.18		
	T44C	p	JPW4039		594	596	0.13	-	0.33		
			JPW4042		634	635	0.06	-	0.30		
			JPW4045		640	636	0.13	-	0.82		
			Acrylodan		499	501	0.01	-	1.52		
			Fluorescein		522	522	0.05	-	0.21	0.64	0.38
			NBD		539	536	0.11	-	0.30	0.006	0.005

Table 5. Spectral and binding parameters of fluorophore-conjugated bPBPs

protein[a]	mutant	site[b]	fluorophore	ligand	$\lambda_{max,\ apo}$	$\lambda_{max,\ sat}$	ΔI_{std} [c]	inc/dec[d]	ΔR_{max} [c]	K_d (μM)	std error
	W315C	p	JPW4039		594	593	0.26	-	0.45	1.00	0.19
			JPW4042		645	640	0.05	-	0.16		
			JPW4045		640	640	0.14	-	0.55	3.2	1.0
			Acrylodan		503	504	0.08	-	0.47	0.13	0.04
			Fluorescein		521	521	0.02	-	0.21		
			NBD		546	546	0.15	-	0.37	0.06	0.02
Glu/Asp BP	A207C	p	JPW4039	glutamate	592	593	0.05	-	0.35		
			JPW4042		635	634	0.20	-	1.37		
			JPW4045		637	639	0.15	-	1.19		
			Acrylodan		498	497	0.26	+	1.61		
			Fluorescein		520	520	0.12	-	0.25		
			NBD		529	542	0.05	+	2.53	119	11
	A210C	p	JPW4039		593	594	0.08	-	0.26		
			JPW4042		648	645	0.11	-	0.79	0.103	0.054
			JPW4045		647	650	0.09	-	0.71		
			Acrylodan		497	496	0.09	-	0.40		
			Fluorescein		522	522	0.02	-	0.14		

Table 5. Spectral and binding parameters of fluorophore-conjugated bPBPs

protein[a]	mutant	site[b]	fluorophore	ligand	$\lambda_{max,\ apo}$	$\lambda_{max,\ sat}$	ΔI_{std} [c]	inc/dec[d]	ΔR_{max} [c]	K_d (μM)	std error
			NBD		543	542	0.02	-	0.30		
	E119C	p	JPW4039		593	594	0.12	+	0.34		
			JPW4045		649	644	0.08	+	**1.73**		
			Acrylodan		498	497	0.11	+	0.65		
			Fluorescein		523	523	0.05	-	0.09		
			NBD		544	544	0.05	-	0.25		
	F126C	a	JPW4039		596	592	0.11	+	0.85		
			JPW4042		642	643	0.01	+	0.40		
			JPW4045		654	643	**0.33**	+	**1.27**	903	94
			Acrylodan		495	482	0.07	+	**2.70**	82	13
			Fluorescein		522	519	0.22	+	**1.73**	1.71 mM	0.13 mM
			NBD		571	572	0.03	+	0.79		
	F131C	a	JPW4039		593	597	0.15	-	0.37	0.151	0.080
			JPW4042		650	643	0.06	-	0.68		
			JPW4045		649	642	0.02	-	0.48		
			Acrylodan		487	492	0.08	-	0.84		
			Fluorescein		522	522	0.05	-	0.13		
			NBD		539	541	0.01	+	0.10		

Table 5. Spectral and binding parameters of fluorophore-conjugated bPBPs

protein[a]	mutant	site[b]	fluorophore	ligand	$\lambda_{max,\ apo}$	$\lambda_{max,\ sat}$	ΔI_{std} [c]	inc/dec[d]	ΔR_{max} [c]	K_d (μM)	std error
	F270C	p	JPW4039		596	594	0.01	-	0.11		
			JPW4042		640	645	0.08	+	0.14		
			JPW4045		644	647	0.07	-	0.69		
			Acrylodan		490	492	0.07	-	0.60		
			Fluorescein		523	523	0.04	-	0.21		
			NBD		572	571	0.06	+	0.31		
	G211C	p	JPW4039		594	592	0.01	+	0.12		
			JPW4042		628	631	0.09	+	0.12		
			JPW4045		631	634	0.06	+	0.36		
			Acrylodan		493	492	0.02	-	0.29		
			Fluorescein		522	521	0.03	-	0.18		
			NBD		538	538	0.07	+	0.32		
	K268C	p	Acrylodan		496	497	0.03	-	0.72		
			Fluorescein		522	522	0.06	-	0.18		
	Q123C	p	JPW4039		592	588	0.05	+	0.75		
			JPW4045		640	641	0.00	-	0.88		
			Acrylodan		498	495	0.10	-	0.40		
			Fluorescein		524	522	0.13	-	2.23	0.75	0.09

Table 5. Spectral and binding parameters of fluorophore-conjugated bPBPs

protein[a]	mutant	site[b]	fluorophore	ligand	$\lambda_{max,\ apo}$	$\lambda_{max,\ sat}$	ΔI_{std} [c]	inc/dec[d]	ΔR_{max} [c]	K_d (μM)	std error
			NBD		544	542	0.01	+	0.53		
	T129C	a	JPW4039		587	584	0.09	+	0.73	0.093	0.015
			JPW4042		649	650	0.06	-	0.68		
			JPW4045		644	648	0.05	-	0.73		
			Acrylodan		484	482	0.04	+	0.52		
			Fluorescein		523	523	0.02	-	0.17		
			NBD		537	538	0.09	+	0.15	0.019	0.011
Fe(III) BP	E203C	p	JPW4039	Fe(III) citrate	599	592	0.09	-	0.37		
			Acrylodan		518	518	**0.41**	-	0.95	138	21
			Fluorescein		523	522	**0.33**	-	0.15	41.9	3.5
			NBD		550	548	**0.31**	-	0.21	221	31
	K202C	p	JPW4039		602	602	0.24	-	0.36	193	29
			Acrylodan		505	503	**0.37**	-	1.17	195	25
			Fluorescein		520	521	**0.30**	-	0.09	195	16
			NBD		542	543	0.23	-	0.14	260	36
	K85C	a	JPW4039		593	591	0.05	-	0.10		
			JPW4042		638	641	0.03	-	0.28		

Table 5. Spectral and binding parameters of fluorophore-conjugated bPBPs

protein[a]	mutant	site[b]	fluorophore	ligand	$\lambda_{max,\ apo}$	$\lambda_{max,\ sat}$	ΔI_{std} [c]	inc/dec[d]	ΔR_{max} [e]	K_d (μM)	std error
			Acrylodan		503	501	0.05	-	0.41		
			Fluorescein		519	520	0.01	-	0.03		
			NBD		545	543	0.08	-	0.12		
	V287C	a	JPW4039		596	595	0.13	-	0.59		
			JPW4042		596	591	0.06	-	0.24		
			Acrylodan		504	506	0.21	-	0.34	221	35
			Fluorescein		521	520	0.21	-	0.05	92.5	7.5
			NBD		551	552	0.05	-	0.11	0.66	0.27
glucose BP	D257C	a	Acrylodan	glucose	505	509	0.18	-	1.97	0.30	0.02
			Fluorescein		523	522	0.07	+	0.41		
			NBD		545	547	0.72	-	0.68	1.39	0.01
			Pyrene		401	402	0.06	+	0.98		
	E149C	p	Acrylodan		525	519	0.60	+	2.26	0.90	0.03
			Fluorescein		527	518	0.32	+	3.63	253	2
			NBD		549	539	*1.74*	+	*2.46*	2.94	0.12
			Pyrene		385	388	0.81	+	2.60	20.2	0.3
	E93C	p	Acrylodan		461	462	0.44	-	2.81	8.74	0.08

Table 5. Spectral and binding parameters of fluorophore-conjugated bI'BI's

protein[a]	mutant	site[b]	fluorophore	ligand	$\lambda_{max,\ apo}$	$\lambda_{max,\ sat}$	ΔI_{std} [c]	inc/dec[d]	ΔR_{max} [c]	K_d (μM)	std error
			Fluorescein		523	521	0.10	+	0.56	0.77	0.03
			NBD		557	546	**0.53**	+	**3.27**	12.3	0.2
			Pyrene		384	385	0.11	+	0.82		
	H152C	e	Acrylodan		527	524	**0.51**	+	**2.97**	48.1	0.5
			Fluorescein		525	519	**0.40**	+	**2.68**	33.7	0.5
			NBD		546	549	**1.29**	+	**1.20**	134	1
			Pyrene		408	389	***1.75***	+	***4.63***	79.3	0.4
	L255C	a	Acrylodan		506	509	**0.57**	-	**1.98**	0.494	0.004
			Fluorescein		525	523	0.23	+	**1.49**	0.159	0.009
			NBD		541	548	0.19	+	**1.71**	0.263	0.021
			Pyrene		387	385	**0.90**	+	0.62	0.133	0.022
	N15C	e	Acrylodan		522	524	0.18	-	0.68	0.21	0.01
			Fluorescein		521	522	0.02	+	0.07		
			NBD		544	547	0.04	-	0.82	0.135	0.007
			Pyrene		400	408	**0.51**	+	**2.62**		
	V296C	a	Acrylodan		501	503	0.00	-	0.63		
			Fluorescein		522	522	0.08	-	0.22	0.216	0.006
			NBD		541	543	**0.40**	-	1.06	0.169	0.011

Table 5. Spectral and binding parameters of fluorophore-conjugated bPBPs

protein[a]	mutant	site[b]	fluorophore	ligand	$\lambda_{max,\ apo}$	$\lambda_{max,\ sat}$	ΔI_{std} [c]	inc/dec[d]	ΔR_{max} [c]	K_d (μM)	std error
			Pyrene		388	392	0.14	+	**3.40**		
	W183C	e	Acrylodan		483	504	**0.73**	-	**5.57**	5.98 mM	0.03 mM
			Fluorescein		525	521	0.10	+	1.16	17.6 mM	2.4 mM
			NBD		547	546	0.13	-	0.14	318 mM	15 mM
			Pyrene		391	390	0.06	-	0.95		
	Y10C	e	Acrylodan		498	497	0.15	-	1.16	116	3
			Fluorescein		521	521	**0.43**	+	1.22	3.31 mM	0.06 mM
			NBD		540	545	0.03	+	**1.28**		
			Pyrene		388	391	0.19	-	**2.87**		
histidine BP	E167C	p	Acrylodan	histidine	504	506	0.17	+	0.72	0.060	0.003
			Fluorescein		517	518	0.08	-	0.40		
			NBD		539	541	0.05	+	0.42		
			Pyrene		384	384	0.21	+	1.13		
	K229C	p	Acrylodan		526	527	0.02	-	0.41		
			Fluorescein		517	516	0.03	-	0.05		
			NBD		532	536	0.12	+	0.31		
			Pyrene		384	384	0.16	+	0.73		

Table 5. Spectral and binding parameters of fluorophore-conjugated bPBPs

protein[a]	mutant	site[b]	fluorophore	ligand	$\lambda_{max,\ apo}$	$\lambda_{max,\ sat}$	ΔI_{std} [c]	inc/dec[d]	ΔR_{max} [c]	K_d (μM)	std error
	V163C	p	JPW4042		659	654	0.82	-	2.44	0.25	0.02
			Acrylodan		493	500	0.03	+	2.05	0.40	0.01
			Fluorescein		520	521	0.12	-	0.10		
			NBD		542	543	0.17	+	1.32	2.37	0.15
			Pyrene		384	384	0.08	+	0.78		
	Y230C	p	Acrylodan		523	522	0.02	-	0.18		
			Fluorescein		517	517	0.05	-	0.07		
			NBD		535	534	0.09	+	0.20		
			Pyrene		384	384	0.22	+	0.75		
	F231C	p	Acrylodan		524	525	0.01	-	0.56		
			Fluorescein		516	516	0.03	+	0.06		
			NBD		545	542	0.07	+	0.19		
	Y88C	a	Acrylodan		491	493	0.03	-	0.30		
			Fluorescein		518	518	0.04	-	0.06		
			NBD		532	532	0.01	-	0.18		
			Pyrene		384	384	0.15	+	0.44		
maltose BP	D95C	a	JPW4039	maltose	591	593	0.08	-	0.70		

Table 5. Spectral and binding parameters of fluorophore-conjugated bPBPs

protein[a]	mutant	site[b]	fluorophore	ligand	$\lambda_{max,\ apo}$	$\lambda_{max,\ sat}$	ΔI_{std} [c]	inc/dec[d]	ΔR_{max} [c]	K_d (μM)	std error
			JPW4042		663	661	0.01	-	0.15		
			JPW4045		650	645	0.08	+	**1.36**	0.30	0.01
			Acrylodan		522	501	0.04	-	**3.31**		
	F92C	a	JPW4039		577	583	**0.43**	-	**1.74**		
			JPW4042		646	646	0.04	-	0.11		
			Acrylodan		495	484	0.16	+	**2.09**		
			Fluorescein		519	518	0.02	+	0.03		
			NBD		531	533	0.09	+	0.27		
	I329C	a	JPW4039		595	594	0.05	-	0.43		
			JPW4042		660	660	0.05	+	0.60		
			JPW4045		652	649	0.04	+	0.55		
			Acrylodan		498	500	0.02	-	0.79		
			Fluorescein		517	518	0.04	+	0.08		
			NBD		522	523	**0.37**	+	**1.33**	0.20	0.02
	S233C	p	JPW4039		577	583	**0.42**	-	**1.73**	145	6
			JPW4042		670	652	**0.87**	-	**4.00**	382	16
			JPW4045		678	657	**0.42**	+	**3.92**	409	22
			Acrylodan		518	519	0.01	-	0.80		

Table 5. Spectral and binding parameters of fluorophore-conjugated bPBPs

protein[a]	mutant	site[b]	fluorophore	ligand	$\lambda_{max,\ apo}$	$\lambda_{max,\ sat}$	ΔI_{std} [c]	inc/dec[d]	ΔR_{max} [c]	K_d (μM)	std error
			Fluorescein		519	519	0.17	+	0.10		
			NBD		544	544	**0.76**	+	0.36	9.3	0.3
phosphate BP	A225C	a	JPW4039	phosphate	591	601	**0.36**	+	**2.86**	0.038	0.019
			JPW4042		615	628	**0.30**	-	**1.32**	0.39	0.08
			JPW4045		621	633	0.02	+	0.82		
			Acrylodan		503	502	0.08	-	**1.95**		
			Fluorescein		522	521	0.01	-	0.97	0.20	0.03
			NBD		544	554	**0.81**	-	1.21	0.27	0.03
	N223C	a	Fluorescein		519	519	0.06	+	0.01		
	N226C	a	JPW4039		595	571	**0.26**	+	**2.94**	0.066	0.054
			JPW4042		673	651	**0.29**	+	**2.05**	0.172	0.148
			JPW4045		675	638	**0.53**	+	**3.83**	0.277	0.169
	S164C	p	JPW4039		599	550	***0.91***	-	***3.39***	0.66	0.03
			JPW4042		630	615	**0.33**	-	**1.78**	1.16	0.22
			JPW4045		645	563	**0.27**	-	**2.99**	0.64	0.06
			Acrylodan		505	503	0.05	+	**3.53**	0.22	0.06

Table 5. Spectral and binding parameters of fluorophore-conjugated bPBPs

protein[a]	mutant	site[b]	fluorophore	ligand	$\lambda_{max,\ apo}$	$\lambda_{max,\ sat}$	ΔI_{std} [c]	inc/dec[d]	ΔR_{max} [c]	K_d (μM)	std error
			Fluorescein		521	520	0.07	+	0.30	0.17	0.02
			NBD		539	540	0.02	+	0.42		
	S39C	p	JPW4039		597	551	0.36	-	**3.15**	0.42	0.06
			JPW4042		623	622	0.01	+	0.15		
			JPW4045		671	647	0.18	-	**4.13**	0.23	0.04
			Acrylodan		520	520	0.10	-	0.80		
			Fluorescein		519	518	0.03	-	0.21		
			NBD		558	559	0.18	+	0.57	0.14	0.04
glutamine BP	N160C	p	Acrylodan	glutamine	529	527	0.11	+	0.43	0.098	0.023
			NBD		546	543	0.09	+	0.71		
			Pyrene		387	387	0.04	-	0.15		
	F221C	p	JPW4042		654	652	0.18	-	0.70		
			Acrylodan		498	498	0.04	-	0.40		
			Fluorescein		518	518	0.02	-	0.10		
			NBD		544	545	0.06	+	0.36	0.0099	0.0034
			NBDE		538	537	0.04	+	0.24		

Table 5. Spectral and binding parameters of fluorophore-conjugated bPBPs

protein[a]	mutant	site[b]	fluorophore	ligand	$\lambda_{max,\ apo}$	$\lambda_{max,\ sat}$	ΔI_{std} [c]	inc/dec[d]	ΔR_{max} [c]	K_d (μM)	std error
	K219C	p	Acrylodan		494	500	**0.25**	-	**1.34**	0.38	0.03
			NBDE		510	510	0.02	+	0.21		
	I.162C	p	Acrylodan		496	501	**0.46**	-	**2.17**	0.17	0.02
			Fluorescein		523	519	0.17	+	**1.80**	0.38	0.06
	W220	p	Acrylodan		519	518	0.03	+	0.58		
			Fluorescein		518	518	0.01	-	0.03		
			NBD		538	538	0.03	-	0.45		
			NBDE		510	510	0.00	-	0.28		
			Pyrene		386	390	**0.40**	+	**2.86**		
	Y163C	p	Acrylodan		503	502	0.07	+	**2.52**	1.40	0.12
			Fluorescein		518	518	0.04	-	0.04		
			NBD		530	528	0.05	-	0.30		
			Pyrene		385	385	0.01	-	0.07		
	Y86C	a	JPW4042		653	653	0.11	-	0.83	0.338	0.038
			Acrylodan		490	484	**0.41**	-	0.49	0.052	0.003
			NBD		541	538	**0.27**	-	0.25		
			NBDE		541	551	0.12	+	**1.81**		

Table 5. Spectral and binding parameters of fluorophore-conjugated bPBPs

protein[a]	mutant	site[b]	fluorophore	ligand	$\lambda_{max,\ apo}$	$\lambda_{max,\ sat}$	ΔI_{std} [c]	inc/dec[d]	ΔR_{max} [c]	K_d (μM)	std error
ribose BP	A234C	a	JPW4039	ribose	598	600	**0.37**	-	**1.29**	1.84	0.40
			JPW4042		668	654	0.06	-	0.99		
			JPW4045		636	578	***0.98***	-	***4.08***	3.76	0.38
			Acrylodan		504	522	0.01	+	1.18		
			Fluorescein		517	517	0.01	-	0.05		
			NBD		546	548	**0.28**	+	**1.63**	0.735	0.057
	D165C	p	JPW4039		589	593	0.13	-	0.36		
			JPW4042		650	652	0.06	-	0.27		
			JPW4045		646	647	0.04	-	0.77		
			Acrylodan		501	500	0.00	-	0.37		
			Fluorescein		522	522	0.03	-	0.37		
	E192C	p	JPW4039		598	598	**0.44**	-	0.34	2.57	0.67
			JPW4042		646	679	***0.99***	-	***4.01***	5.03	0.77
			JPW4045		646	666	***0.89***	-	***2.47***	15.0	0.4
			Acrylodan		516	516	0.04	-	0.27		
			Fluorescein		526	523	0.12	+	**1.31**	11.4	0.8
			NBD		546	540	0.00	+	**1.67**	2.60	0.26
	L236C	a	JPW4039		589	588	0.08	-	0.29		

Table 5. Spectral and binding parameters of fluorophore-conjugated bPBPs

protein[a]	mutant	site[b]	fluorophore	ligand	$\lambda_{max,\ apo}$	$\lambda_{max,\ sat}$	ΔI_{std} [c]	inc/dec[d]	ΔR_{max} [c]	K_d (μM)	std error
			JPW4042		646	670	**0.55**	-	**3.58**	0.62	0.22
			JPW4045		643	658	**0.25**	-	**1.70**	1.53	0.41
			Acrylodan		518	518	0.09	-	0.71		
			Fluorescein		520	520	0.02	-	0.29		
			NBD		518	525	0.11	+	**1.96**	0.10	0.05
	L265C	a	JPW4039		600	596	0.01	-	0.11		
			JPW4042		650	654	**0.91**	-	**2.13**	0.26	0.06
			JPW4045		669	663	0.02	-	0.12		
			Acrylodan		500	501	0.20	-	0.70		
			NBD		545	540	0.01	+	0.13		
	T135C	p	JPW4039		606	606	0.02	-	0.03		
			JPW4042		680	674	0.02	+	0.35		
			JPW4045		647	664	***0.89***	-	***2.45***	>1 mM	
			Acrylodan		518	498	**0.31**	+	**6.26**	0.42 mM	0.01 mM
			Fluorescein		526	523	0.18	+	**1.79**	2.09 mM	0.27 mM
			NBD		542	544	0.08	+	0.22		
sulfate BP	L65C	p	JPW4042	sulfate	629	635	**0.40**	-	**1.82**		

Table 5. Spectral and binding parameters of fluorophore-conjugated bPBPs

protein[a]	mutant	site[b]	fluorophore	ligand	$\lambda_{max,apo}$	$\lambda_{max,sat}$	ΔI_{std} [c]	inc/dec[d]	ΔR_{max} [c]	K_d (μM)	std error
			Acrylodan		492	482	0.39	+	2.95		
			Fluorescein		520	516	0.39	+	1.31	1.09	0.05
			NBD		522	521	0.02	-	0.61		
			Pyrene		386	385	0.13	+	1.20		
	N70C	p	JPW4042		522	522	0.01	+	0.18		
			Acrylodan		502	502	0.01	-	0.10		
			Fluorescein		517	517	0.01	-	0.01		
			NBD		524	524	0.01	-	0.14		
			Pyrene		386	386	0.01	-	0.13		
	Q294C	p	JPW4042		636	630	0.27	-	1.17	0.83	0.08
			Acrylodan		500	500	0.04	-	0.13		
			Fluorescein		515	514	0.00	+	0.11		
			NBD		530	530	0.00	+	0.02		
			Pyrene		384	384	0.01	+	0.08		
	R134C	p	JPW4039		522	518	0.08	-	2.02	7.5	0.2
			JPW4042		606	608	0.52	+	0.96	29.1	1.2
			Acrylodan		493	478	0.18	-	2.26	4.17	0.13
			Fluorescein		512	512	0.01	-	0.02	0.323	0.027

Table 5. Spectral and binding parameters of fluorophore-conjugated bPBPs

protein[a]	mutant	site[b]	fluorophore	ligand	$\lambda_{max,\ apo}$	$\lambda_{max,\ sat}$	ΔI_{std} [c]	inc/dec[d]	ΔR_{max} [c]	K_d (μM)	std error
			NBD		531	532	**0.58**	-	0.37	22.4	0.5
			Pyrene		382	386	0.15	+	**1.30**		
	W290C	p	JPW4042		612	624	**0.43**	-	0.89	0.336	0.012
			Acrylodan		496	496	0.04	-	0.03		
			Fluorescein		516	515	0.04	+	0.09		
			NBD		538	537	0.06	-	0.11		
			Pyrene		384	384	0.16	+	0.37		
	Y67C	p	Acrylodan		503	502	0.00	-	0.12		
			Fluorescein		515	515	0.01	-	0.04		
			NBD		536	534	0.13	+	0.20		
			Pyrene		383	383	0.02	+	0.48		

a: All mutants of arabinose BP were in the C64A background.
All mutants in Fe(III) BP were in the E57D background.

b: a: allosteric, e: endosteric, p: peristeric

c: Numbers in bold meet the threshold criteria of sensor utility elaborated in the text.
Underlined numbers indicate excellent absolute intensity or ratiometric sensors.
Numbers in bold italic are excellent sensors in both parameters.

d: inc/dec, increase (+) or decrease (-) in maximum fluorescence intensity upon ligand binding.

Assessment of fluorescent biosensor function. Fluorescence emission spectra of bPBP-fluorophore conjugates were recorded in the absence and presence of saturating ligand concentrations. Spectral changes were characterized by four parameters: wavelength shift (the difference between the wavelengths of emission maximum in the unbound and ligand-saturated states), direction of intensity change (increase or decrease in intensity at the wavelengths of maximum emission in the two states), standard intensity change (ΔI_{std}), and standard ratiometric change (ΔR). ΔI_{std} is defined as the normalized intensity change relative to the average intensity, determined at the wavelength mid-point between the two emission maxima:

$$\Delta I_{std} = \left| \frac{2(I_1(\lambda_{std}) - I_2(\lambda_{std}))}{I_1(\lambda_{std}) + I_2(\lambda_{std})} \right| \quad (1)$$

where $\lambda_{std} = (\lambda_{max,\ unbound} + \lambda_{max,\ saturated})/2$ and I_1, I_2 are the fluorescence intensities at λ_{std} of each spectrum respectively (Fig 4A). ΔR is defined in terms of two emission bands, A_1 ($[\lambda_1, \lambda_2]$) and A_2 ($[\lambda_3, \lambda_4]$) (Fig 4B):

$$\Delta R = \left| \frac{{}^0A_1}{{}^0A_2} - \frac{{}^\infty A_1}{{}^\infty A_2} \right| \quad (2)$$

where ${}^0A_1$, ${}^\infty A_2$ are the areas in the absence of ligand, and ${}^\infty A_1$, ${}^\infty A_2$ the areas in the presence of saturating ligand. A computer program was used to enumerate ΔR for all possible pairs of wavelength bands in the two spectra, to identify the optimal sensing condition, defined as the maximum value of ΔR. Adjustable parameters of the algorithm, and their values used for ΔR_{max} quantities reported here, are: step size (2 nm), step width (10 nm), minimum integration area limit (fraction of total: 0.1), and maximum integration area limit (fraction of total: 1).

Analyte affinity measurements. 133 bPBP-fluorophore conjugates with $\Delta I_{std} > 0.1$ were used to determine ligand binding affinity by fluorimetric titration (Table 5). The emission wavelength monitored was that of maximum difference in intensity between the ligand-free and bound states. For each conjugate, fluorescence intensiometric observations were fit to a hyperbolic binding isotherm for a two-state model (Marvin et al., Proc. Natl. Acad. Sci. USA 94:4366-4371, 1997):

$$F = \frac{K_d F_F + [S]F_B}{K_d + [S]} \quad (3)$$

where F is fluorescence at ligand concentration [S], K_d is the dissociation constant, and F_F, F_B are the fluorescence intensities of the ligand-free and ligand-saturated states, respectively. Examples of binding isotherms are shown in Figure 5 for glucose BP and glutamate/aspartate BP. For ratiometric observations, eq. 3 has to be modified to account for differentially weighted contributions of the two emission bands (Lakowicz, *Principles of Fluorescence Spectroscopy, 2nd Ed.* Kluwer Academic Press, New York, p. 698, 1999):

$$R = \frac{^{app}K_d R_F + [S]R_B}{^{app}K_d + [S]} \quad (4)$$

where R is ratio A_1/A_2, $R_B = {}^{\infty}A_1/{}^{\infty}A_2$, $R_F = {}^{0}A_1/{}^{0}A_1$, and $^{app}K_d$ is an apparent dissociation constant:

$$^{app}K_d = \frac{^{0}A_2}{^{\infty}A_2} K_d \quad (5)$$

The success of the fluorescent biosensor design strategy was evaluated by determining the probability of encountering an effectively responding fluorescent conjugate, and assessing how the ligand-binding affinities are affected by the fluorophore conjugate.

Assessment of ligand-mediated changes in fluorescence. Summaries of wavelength shift, ΔI_{std}, and ΔR_{max} for all conjugates (n=320) are presented as histograms in Figure 6A. The distribution of wavelength shifts was symmetrical about zero; that is, there was no overall tendency toward either blue- or red- shifts. Of the entire collection of conjugates, 130 show increases and 190 show decreases in fluorescence intensity upon binding. A portion of this skew is due to the finding that addition of Fe(III) citrate to all Fe(III) BP conjugates caused a decreased fluorescence emission. To examine whether this was due to quenching by Fe(III) in solution, Fe(III) citrate was added to conjugates of other bPBPs and the effect on emission intensity was monitored. It was found that Fe(III) citrate quenched fluorescence in all cases, but only at concentrations much higher than those that led to the effect in Fe(III) BP. The decrease in fluorescence intensity observed in all conjugates of Fe(III) BP is therefore due to a binding-specific process, and may involve relaxation of the excited state via a metal-mediated redox mechanism (Lakowicz,

Principles of Fluorescence Spectroscopy, 2nd Ed. Kluwer Academic Press, New York, p. 698, 1999). The probability of encountering a conjugate that responds with a particular intensity declines with increasing magnitude of ΔI_{std} (Fig 6B). The ratiometric response behaves similarly (Fig. 6C).

The two criteria of greatest utility for optical sensing are ΔI_{std} and ΔR_{max}. The collection of bPBP conjugates was categorized by class of steric site, fluorophore, and protein scaffold, then, for each category, quantified according to the fraction with $\Delta I_{std} > 0.25$ and with $\Delta R_{max} > 1.25$. The results (Tables 6 to 8) give an indication of the overall success rate for finding potentially useful fluorescent biosensor conjugates. For the collection of 320 conjugates, about 24% meet the criterion for ΔI_{std} and about 28% the criterion for ΔR_{max}.

Table 6. Signaling parameters by binding protein

binding protein	fraction $\Delta I_{std}>0.25$	fraction $\Delta R_{max}>1.25$	n
arabinose BP	0.50	0.40	20
glucose BP	0.47	0.50	36
ribose BP	0.32	0.41	34
dipeptide BP	0.08	0.14	36
glutamine BP	0.20	0.24	25
histidine BP	0.04	0.13	24
Glu/Asp BP	0.04	0.15	54
phosphate BP	0.45	0.55	22
sulfate BP	0.23	0.20	30
maltose BP	0.29	0.38	21
Fe(III) BP	0.28	0.00	18
aggregate	0.24	0.28	320

Table 7. Signaling parameters by steric site

site	fraction $\Delta I_{std}>0.25$	fraction $\Delta R_{max}>1.25$	n
allosteric	0.28	0.32	110
peristeric	0.20	0.15	198
endosteric	0.50	0.50	12
aggregate	0.24	0.28	320

Table 8. Signaling parameters by fluorophore

fluorophore	fraction $\Delta I_{std}>0.25$	fraction $\Delta R_{max}>1.25$	n
Acrylodan	0.21	0.38	66
Fluorescein	0.13	0.16	62
NBD	0.25	0.20	61
NBDE	0.00	0.25	4
Pyrene	0.22	0.30	23
JPW4039	0.38	0.28	39
JPW4042	0.32	0.30	37
JPW4045	0.29	0.39	28
aggregate	0.24	0.28	320

There appears to be a correlation between signaling success rate and the sequence-related family, or cluster (Tam & Saier, Microbiol. Rev. 57:320-346, 1993), to which a scaffold belongs. The scaffolds having the highest success rates for ΔI_{std} and ΔR_{max} are arabinose BP, glucose BP, ribose BP, and phosphate BP (Table 6). The former three belong to cluster 2, that includes binding proteins for hexoses and pentoses, while phosphate BP, along with sulfate BP, belongs to cluster 6, that includes binding proteins for inorganic polyanions. The scaffolds having the lowest success rate were dipeptide BP (cluster 5, peptide and nickel binding) and the cluster 3 (polar amino-acid binding) proteins glutamine BP, histidine BP, and Glu/Asp BP.

Among the three classes of attachment sites the endosteric and allosteric sites have a higher chance of meeting the threshold criteria than peristeric sites (Table 7). Success rates in terms of ΔI_{std} varied according to the environmental sensitivity of the fluorophore, being highest with the styryl and naphthyl dyes JPW4039, JPW4042, and JPW4045. Similarly, higher success rates for ΔR_{max} were associated with JPW4045 and acrylodan (Table 8).

Assessment of changes in ligand-binding affinities. The range of dissociation constants, K_d, extracted from the binding curves for each ligand is shown in Table 9. Since there is a thermodynamic linkage between ligand binding and the interaction of the attached fluorophore with the protein, the fluorophore is expected to change the intrinsic ligand dissociation constant. The change in affinity imparted by the flourophore is expected to be dependent on its location in the protein. The various conjugates exhibit a wide range of affinities (Table 9). The change in affinity, defined as $\log({}^{mut}K_d/{}^{wt}K_d)$, was examined as a function of attachment site classification (endosteric, allosteric, or peristeric) among the 108 conjugates for which dissociation constants were measured and for which the dissociation constant of the unconjugated protein is known (Table 2). The results reveal that the three classes of site have different effects on affinity (Fig. 7). Fluorophore attachment at endosteric sites tends to perturb affinity the greatest, and uniformly to higher values of K_d than the wild type. Allosteric and peristeric attachment results in K_d values that are either higher or lower than the wild type, with peristeric sites exhibiting the greatest variation in effects. Interestingly, of those conjugates with higher affinity than the wild type (lower K_d), a greater proportion derives from conjugation at allosteric sites. This corroborates detailed studies in maltose BP in which affinity was increased by manipulating the volume of residues in allosteric sites (Marvin & Hellinga, Nat. Struct. Biol. 8:795-798, 2001). The differences in effects can be rationalized in terms of the likelihood that a particular conjugate will sterically interfere either directly with ligand binding (endosteric sites, and some peristeric sites), or by influencing the intrinsic equilibrium between the open and closed states (allosteric sites, peristeric sites).

Table 9. Range of ligand affinities in bPBP fluorescent conjugates

bPBP	ligand	range of K_d(μM)	n
arabinose BP	arabinose	0.46 - 775	19
glucose BP	glucose	0.13 - 318000	26
ribose BP	ribose	0.1 - 2090	14
dipeptide BP	Gly-Leu	0.006 - 93	21
glutamine BP	glutamine	0.01 - 1.4	8
histidine BP	histidine	0.06 - 2.37	4
Glu/Asp BP	glutamate	0.019 - 1700	9
phosphate BP	phosphate	0.038 - 1.2	12
sulfate BP	sulfate	0.32 - 29	8
maltose BP	maltose	0.2 - 409	6
Fe(III) BP	Fe(III) citrate	0.66 - 260	10

The effect on dissociation constants is determined not only by the attachment site, but also by the nature of the attached fluorophore, as illustrated for arabinose BP. Dissociation constants for arabinose of the five cysteine-substitution mutants (all with the C64A mutation), measured by tryptophan fluorescence, are 5.0 μM (F23C), 3.2 μM (L253C), 3.4 μM (D257C), 7.6 μM (L298C), and 1.6 μM (K301C). Thus the cysteine substitutions slightly perturbed affinity for arabinose (K_d of C64A mutant ~ 2.2 μM). The largest dependence on the attached fluorophore was found for the L253C mutant, for which K_d values ranged from 0.7 μM (acrylodan) to 775 μM (NBD). Similarly, the K394C mutant of dipeptide BP has affinities for Gly-Leu dipeptide ranging from 6 nM (NBD) to 93 μM (fluorescein). Most mutants did not exhibit such a wide range of fluorophore-dependent ligand affinity. For example, five different fluorophores conjugated to ribose BP E192C have affinities for ribose ranging from 2.6 μM (NBD and JPW4039) to 15 μM (JPW4045).

Construction of a novel biosensor using sequence information. To demonstrate that designs are not limited to those bPBPs with known structure, cysteine mutations were introduced into a paralog predicted to code for a glutamate/aspartate BP, using histidine and glutamine BPs as the structures to guide locations for likely peristeric and allosteric sites. All the ten sites that were tried yielded conjugates that exhibited glutamate and aspartate-dependent changes in fluorescence. Several sites yielded good or excellent intensiometric or ratiometric sensors. Table 10 shows that the response is specific for both aspartate and glutamate, with 50- to 500-fold weaker affinity for glutamine and asparagine. Other amino acids and sugars did not elicit ligand-mediated changes in fluorescence.

Table 10. Binding specificity and affinity in mutants of glutamate/aspartate BP

		$K_d(\mu M)$			
mutant	fluorophore	Glu	Asp	Gln	Asn
Q123C	Fluorescein	0.75	1.8	49	96
F126C	Acylodan	82	115		
F126C	Fluorescein	1707	2000		
F126C	JPW4045	903	1497		
T129C	NBD	0.019	0.061	12.1	5.4
T129C	JPW4039	0.093	0.035	23	
F131C	JPW4039	0.15			
A207C	NBD	119	454		
A210C	JPW4042	0.10			

Bioinformatics makes possible the discovery of new biochemical applications without direct experimentation. In the case of biosensors, individual bacterial genomes may encode scores of bPBPs that bind specific molecules to initiate transport or signal transduction (Blattner et al., Science 277:1453-1474, 1997; Quentin et al., J. Mol. Biol. 287:467-484, 1999). Few of these have been characterized, leaving a vast number

untapped as scaffolds for potential biosensors. The feasibility of applying genomic information, combined with structural information from homologous proteins, to construct a biosensor of novel specificity has been demonstrated.

Previously, a glutamate/aspartate BP had been purified from *E. coli* (Barash & Halpern, Biochim. Biophys. Acta 386:168-180, 1975; Willis & Furlong, J. Biol. Chem. 250:2574-2580, 1975) and characterized. Several pieces of evidence suggest that YBEJ corresponds to this protein. First, glutamate/aspartate BP was isolated from periplasmic extracts, consistent with *ybeJ* encoding a protein with a putative periplasmic localization signal sequence. Second, the previously determined molecular mass of glutamate/aspartate BP of 32 kDa (Barash & Halpern, Biochim. Biophys. Acta 386:168-180, 1975) or 31 kDa (Willis & Furlong, J. Biol. Chem. 250:2574-2580, 1975) matches the mass of 32.5 kDa predicted for the processed *ybeJ* product, and the mass of 30 kDa found by gel electrophoresis in the present study. Third, the amino acid compositions determined previously (Barash & Halpern, Biochim. Biophys. Acta 386:168-180, 1975; Willis & Furlong, J. Biol. Chem. 250:2574-2580, 1975) are similar to that predicted from the gene sequence, with some deviations due likely to inherent inaccuracy in analysis of protein acid hydrolyzates. Finally, the reported K_d values for glutamate (0.8 μM), aspartate (1.2 μM), as well as the relatively lower affinity for glutamine and asparagine (Willis & Furlong, J. Biol. Chem. 250:2574-2580, 1975) are similar to those determined here, and comparable to the Q123C-fluorescein conjugate (Table 10). Hence, *ybeJ* likely encodes the glutamate/aspartate BP previously characterized.

Effective sensor designs. The utility of a conjugate is determined by the absolute change in signal intensity, the ratiometric change, and the operating concentration range over which the sensor can respond accurately. Of the two observable parameters, ratiometric change is preferable to absolute intensities, since it is independent of probe concentration.

Although usable conjugates can be defined as having $\Delta I_{std} > 0.25$ and $\Delta R_{max} > 1.25$, "excellent" sensors can be defined as having $\Delta I_{std} > 0.9$ and $\Delta R_{max} > 2.5$. The magnitudes of the changes in the excellent sensors are likely to be sufficiently large to permit robust measurements in "real-world" applications in complex fluids such as blood. Based on these criteria there are only thirteen excellent absolute intensity-based sensors (4% of total), but 36 excellent ratiometric sensors (11% of total); there are seven

conjugates that are both excellent absolute intensity and excellent ratiometric sensors (Table 5). With the exception of dipeptide BP, Fe(III) BP, and histidine BP, all the proteins have at least one excellent ratiometric and intensity-based conjugate. Glucose BP has the largest number of excellent conjugates. These conjugates all involve fluorophores known to be particularly environmentally sensitive (acrylodan, NBD, pyrene, and the styryl dyes). The incidence of excellent sensors is evenly distributed between allosteric and peristeric sites. All endosteric sites give rise to excellent sensors.

The dissociation constant of a conjugate determines the operating concentration range over which the sensor can respond accurately. The operating range guaranteed to give less than a 5% error spans concentrations that fall within five-fold of the K_d value (Marvin et al., Proc. Natl. Acad. Sci. USA 94:4366-4371, 1997). If the range required for accurate determination is wider than that span, then a composite biosensor can be constructed using receptors of varying affinities, as has been demonstrated for maltose BP (Marvin et al., Proc. Natl. Acad. Sci. USA 94:4366-4371, 1997). There are three factors affecting the dissociation constant: the nature of the conjugate, the choice of emission bands for a ratiometric sensor (eq. 2), and additional mutations. For particular applications, these three factors can be manipulated to construct an appropriate sensor.

Glucose sensor. Among the analytes applicable to clinical medicine, glucose is one of the most important, particularly with regard to diagnosing and treating diabetes. The normal range of glucose concentration in adult human serum is 4 to 6 mM (Burtis & Ashwood, *Teitz Textbook of Clinical Chemistry, 2nd Ed.* W.B. Saunders Co., Philadelphia, Pennsylvania, 1994). The acrylodan conjugate of the endosteric site W183C in glucose BP has an excellent ratiometric response (ΔR_{max} = 5.57) and a dissociation constant of 5.98 mM, and is therefore a good candidate for detecting glucose fluctuations in the physiological range by ratiometry (Figure 8A). Furthermore, by adjusting the ratiometric parameters, the observation window is easily extended from 5.0 to 17.4 mM, allowing all clinically relevant ranges to be observed with one sensor (Figure 8A).

Other sensors for clinical chemistry. Amino acids are also commonly assayed in clinical tests as indicators of disease states. Histidine is an indicator of histidase deficiency (Taylor et al., Molec. Biol. Med. 8:101-116, 1991). The best signaling histidine BP conjugate, V163C-JPW4042, has a K_d of 0.25 μM, below the normal range in serum of about 48 to 125 μM. However, with sample dilution this conjugate could function

effectively. Alternatively the K_d can be adjusted by mutagenesis as was done for maltose BP (Marvin & Hellinga, Nat. Struct. Biol. 8:795-798, 2001) and Fe(III) BP with the E57D mutation. The neuroexcitatory amino acid glutamate has normal serum concentrations of 20 to 220 μM (Burtis & Ashwood, *Teitz Textbook of Clinical Chemistry, 2nd Ed.* W.B. Saunders Co., Philadelphia, Pennsylvania, 1994). The best-suited biosensor is glutamate/aspartate BP F126C-acrylodan, which has a $K_d \sim 80$ μM and $\Delta R_{max} = 2.70$. Glutamine is often measured in cerebrospinal fluid (Smith & Forman, Clin. Lab. Sci. 7:32-38, 1994) in which its normal range is 120 to 360 μM, considerably higher than the K_d (~ 1.4 μM) of the best-signaling glutamine BP conjugate, Y163C-acrylodan. This biosensor can be used for such a purpose by mutagenesis to adjust the K_d, or by sample dilution.

Phosphate concentrations in serum and urine are clinically relevant (Burkhardt et al., Am. J. Clin. Pathol. 72:326-329, 1979). Several phosphate BP conjugates signal well, the best being S39C-JPW4045, and their K_d values are all less than 2 μM. Inorganic phosphate in serum is typically 1 to 3 mM (Burtis & Ashwood, *Teitz Textbook of Clinical Chemistry, 2nd Ed.* W.B. Saunders Co., Philadelphia, Pennsylvania 1994), requiring adjustment of the K_d or sample dilution for accurate measurements with these sensors.

Maltose concentration is relevant to a deficiency in acid maltase, with the normal plasma concentration about 2 μM (Rozaklis et al., Clin. Chem. 48:131-139, 2002). The best maltose sensors in the present work are maltose BP conjugates S233C-JPW4042 ($\Delta R_{max} = 4.0$) and S233C-JPW4045 ($\Delta R_{max} = 3.9$), both with similar affinities ($K_d \sim 400$ μM). Fluorescent conjugates of maltose BP mutants having affinities in the 2 μM range have been described by Marvin et al. (Proc. Natl. Acad. Sci. USA 94:4366-4371, 1997).

Industrial and environmental applications. bPBP conjugates can function as sensors for industrial and environmental analytes. Arabinose is relevant to improving the efficiency of ethanol production from corn (Deanda et al., Appl. Environ. Microbiol. 62:4465-4470, 1996). Of the arabinose BP conjugates, the best signalers are K301C-NBD ($K_d \sim 31$ μM, $\Delta R_{max} = 3.2$) and L253C-fluorescein, ($K_d \sim 48$ μM, $\Delta R_{max} = 2.7$). Ribose concentration, assayed in foods and beverages (AOAC, *Official Methods of Analysis of AOAC International, 16th Ed.* AOAC International, Arlington, Virginia, 1995), can be measured by ribose BP conjugates T135C-acrylodan ($K_d \sim 0.4$ mM, $\Delta R_{max} = 6.3$) and A234C-JPW4045 ($K_d \sim 3.8$ μM, $\Delta R_{max} = 4.1$). Ratiometric sensing of ribose using a single ribose BP derivative is illustrated by the T135C-acrylodan conjugate (Fig. 8B). By varying

emission wavelength bands in the fluorescence ratio (eqs. 4, 5) the $^{app}K_d$ for ribose can be adjusted over a range from 41 to 146 μM (Fig. 8B). Sulfate concentrations in drinking water are of concern (U.S. EPA, *Health Effects From Exposure to High Levels of Sulfate in Drinking Water*, pp. 1-25, Office of Drinking Water and Ground Water, 1999), and can be analyzed by sulfate BP conjugate R134C-acrylodan (K_d ~ 4 μM, ΔR_{max} = 2.3). High concentrations of phosphate are environmentally deleterious, and could be monitored using phosphate BP conjugates, as noted above for clinical applications. Iron concentration limits primary productivity in certain regions of the oceans (Martin, *Iron as a Limiting Factor in Primary Productivity and Biogeochemical Cycles in the Sea*. Falkowski & Woodhead, eds., pp. 123-137, Plenum Press, New York). Available ferric ion can be determined using a biosensor derived from Fe(III) BP, such as conjugate E203C-acrylodan (K_d ~ 138 μM, ΔI_{std} 0.4).

* * *

All documents cited above are hereby incorporated in their entirety by reference. Also incorporated by reference for their disclosure of electronic devices containing bioelectronic sensors are U.S. Appln. No. 10/229,286 (published as US 2003/0129622) and Int'l Appln. No. PCT/US02/27279 (WO 03/021247).

WE CLAIM:

1. A biosensor for ligand, which comprises a bacterial periplasmic binding protein (bPBP) which is not maltose binding protein and at least one reporter group attached at one or more specific positions of said bPBP; wherein binding of said ligand in a ligand-binding pocket of said biosensor causes a change in signaling by said reporter group; with the proviso that a biosensor comprising a glucose binding protein (GBP) is limited to attaching at least one reporting group at one or more positions of said GBP selected from the group consisting of 10, 93, 149 and 183.

2. The biosensor according to claim 1, wherein said bPBP is selected from the group consisting of arabinose binding protein (ABP), ribose binding protein (RBP), dipeptide binding protein (DBP), glutamine binding protein (QBP), histidine binding protein (HBP), glutamate/aspartate binding protein (EBP), phosphate binding protein (PBP), sulfate binding protein (SBP), and Fe(III) binding protein (FeBP).

3. The biosensor according to claim 1 or 2, wherein said bPBP is comprised of one or more mutations at a position(s) where said reporting group is not covalently linked.

4. The biosensor according to claim 1 or 2, wherein said ligand-binding pocket is comprised of one or more mutations and said ligand does not bind to wild-type bPBP.

5. The biosensor according to any one of claims 1-4, wherein said reporter group is attached to said bPBP at one or more positions at a distance from said ligand-binding pocket.

6. The biosensor according to any one of claims 1-4, wherein said reporter group is attached to said bPBP at one or more positions proximal to said ligand-binding pocket.

7. The biosensor according to any one of claims 1-6, wherein said reporter group is covalently attached at one or more specific positions of said bPBP.

8. The biosensor according to any one of claims 1-6, wherein said reporter group is noncovalently attached at one or more specific positions of said bPBP.

9. The biosensor according to any one of claims 1-8, wherein said reporter group is a redox cofactor.

10. The biosensor according to any one of claims 1-7, wherein said reporter group is a fluorophore.

11. The biosensor according to claim 10, wherein said biosensor's standard intensity change (ΔI_{std}) upon binding of ligand is greater than 0.25.

12. The biosensor according to claim 11, wherein said ΔI_{std} is greater than 0.9.

13. The biosensor according to claim 10, wherein said biosensor's maximum value of standard ratiometric change (ΔR_{max}) upon binding of ligand is greater than 1.25.

14. The biosensor according to claim 13, wherein said ΔR_{max} is greater than 2.5.

15. A biosensor for ligand, which comprises a bacterial periplasmic binding protein (bPBP) and at least one reporter group attached at one or more specific positions of said bPBP which are episteric or endosteric sites.

16. Use of a biosensor according to any one of claims 1-15 to assay for ligand.

17. A method of detecting presence or absence of ligand in a sample, which comprises: contacting a biosensor according to any one of claims 1-15 with said sample under conditions such that said biosensor is able to bind to ligand present in said sample; comparing the signal transduced by said reporter group when said biosensor is contacted with said sample with the signal(s) transduced by said reporter group when said biosensor is contacted with at least one control sample containing a known quantity of ligand; and determining the presence or absence of ligand in said sample from said comparison.

18. A method of quantitating amount or concentration of ligand in a sample, which comprises: contacting a biosensor according to any one of claims 1-15 with said sample under conditions such that said biosensor is able to bind to ligand present in said sample; comparing the signal transduced by said reporter group when said biosensor is contacted with said sample against signals transduced by a series of control samples containing known quantities of ligand; and calculating the quantity of ligand in said sample from said comparison.

19. A method of assaying for ligand in a sample, which comprises:

(a) contacting a biosensor comprised of a bacterial periplasmic binding protein (bPBP) and at least one reporter group attached at one or more specific positions of said bPBP with said sample, wherein binding of said ligand in a ligand-binding pocket of said biosensor causes a change in signaling by said reporter group;

(b) measuring a ratiometric change (ΔR) for the signal transduced by said reporter group; and

(c) at least detecting or quantitating ligand present in said sample.

20. The method of any one of claims 17-19, wherein said sample is comprised of a physiological fluid.

21. The method of claim 20, wherein said physiological fluid is selected from the group consisting of blood, interstitial fluid, lavage, perspiration, plasma, saliva, serum, and urine.

22. The method of any one of claims 17-19, wherein said sample is suspected of being comprised of a ligand selected from the group consisting of amino acids, bioactive solid and gaseous compounds which are soluble, carbohydrates, contraband or controlled substances, environmental pollutants, explosives, food contaminants and byproducts, lipids, metal ions, microbial toxins, neurotransmitters, nucleosides or nucleotides, peptides, steroids, and therapeutic drugs.

23. A method of constructing a biosensor, which comprises:

(a) selecting a first bacterial periplasmic binding protein (bPBP) of known amino acid sequence, wherein said first pPBP's three-dimensional structure has not been solved;

(b) modeling said first bPBP's three-dimensional structure on a three-dimensional structure which has been solved for a second bPBP;

(c) aligning at least one allosteric, endosteric, or peristeric site of said second bPBP with one or more putative positions at which reporter groups are to be attached to said first bPBP; and

(d) attaching at least one reporter group at one or more of said putative positions of said first bPBP to form a putative biosensor and determining whether said putative biosensor is functional.

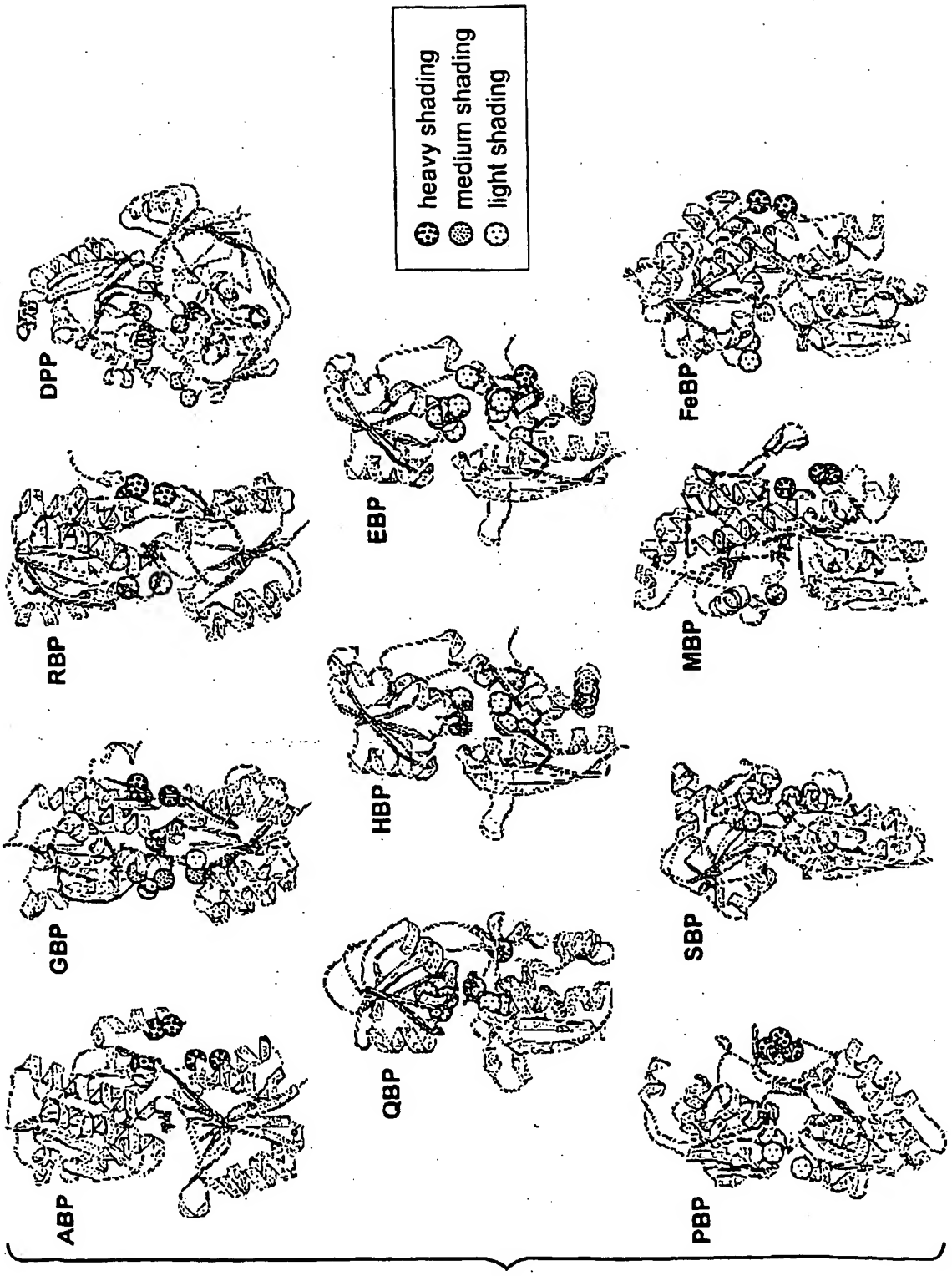
heavy shading
medium shading
light shading
DPP
FeBP
EBP
RBP
MBP
HBP
GBP
SBP
QBP
ABP
PBP

Fig. 1

```
                47                  67                  87                 107                 127
gln BP  ----------ADKKLVVATD TAFVPFEFKQGD-KYVGFDV DLWAAIAKELK-------LD YELKPMDFSGIIPALQTKNV DLALAGITITDERKKAIDFS
his BP  ----------AIPQNIRIGTD PTYAPFESKNSQGELVGFDI DLAKELCKRIN-------TQ CTFVENPLDALIPSLKAKKI DAIMSSLSITEKRQQEIAFT
   YBEJ MAGSTLDKIAKNGVIVVGHR ESSVPFSYYDNQQKVVGYSQ DYSNAIVEAVKKKLNKPDLQ VKLIPITSQNRIPLLQNGTF DFECGSTTNNVERQKQAAFS
                                                                                          p   p   a

               147                 166                 186                 206                 226
gln BP  DGYYKSGLLVMVKANNNDVK SVKDLDGKVVAVKSGTGSVD YAKANIKTK--DLRQFPNID N--AYMELGTNRADAVLIDT PNILY-FIKTAGNGQFKAVG
his BP  DKLYAADSRLVVAKNSDIQP TVESLKGKRVGVLQGTTQET FGNEHWAPKGIEIVSYQGQD N--LYSDLTAGRIDAAFQDE VAASEGFLKQPVGKDYKFGG
   YBEJ  DTIFVVGTRLLTKKGGD-IK DFANLKDKAVVVTSGTTSEV LLNKLNEEQKMNMRIISAKD HGDSFRTLESGRAVAFMMDD ALLAGERAKAKKPDNWEIVG
          a a                                                                                 pp pp

               241                 261                 281                 301
gln BP  DSLEAQQYG-----IAFPKG SDELRDKVNGALKTLRENGT YNEIYKKWFGTEPK------ ---------------------- -
his BP  PSVKDEKLFGVGTGMGLRKE DNELREALNKAFAEMRADGT YEKLAKKYFDFDVYGG---- ---------------------- -
   YBEJ  KPQSQEAYG-----CMLRKD DPQFKKLMDDTIAQVQTSGE AEKWFDKWFKNPIPPKNLNM NFELSDEMKALFKEPNDKAL N
                                                                ppp
```

Fig. 2

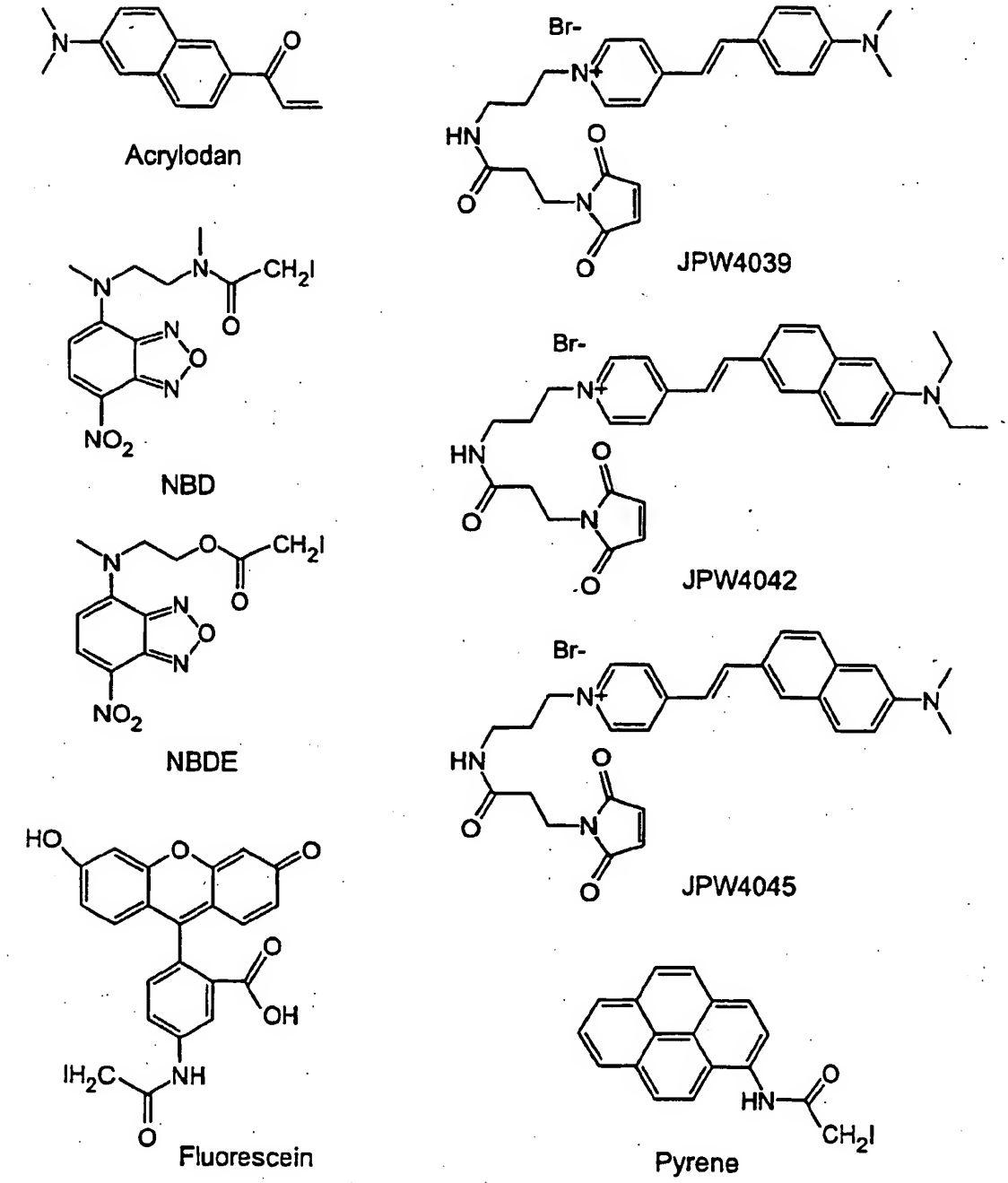
Acrylodan
NBD
NBDE
Fluorescein
JPW4039
JPW4042
JPW4045
Pyrene

Fig. 3

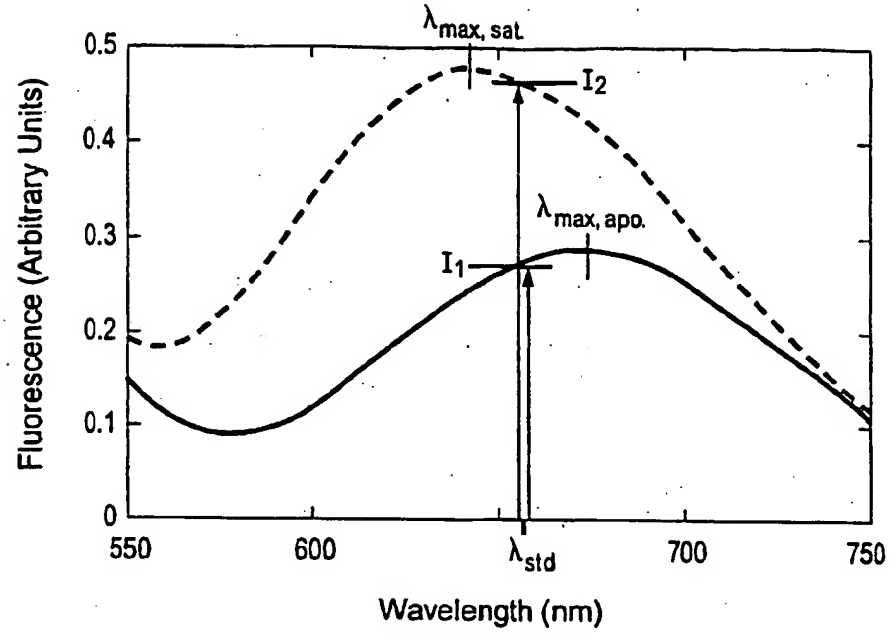
λmax, sat.
I2
λmax, apo.
I1
0.5
0.4
0.3
0.2
0.1
0
550
600
λstd
700
750
Fluorescence (Arbitrary Units)
Wavelength (nm)

Fig. 4A

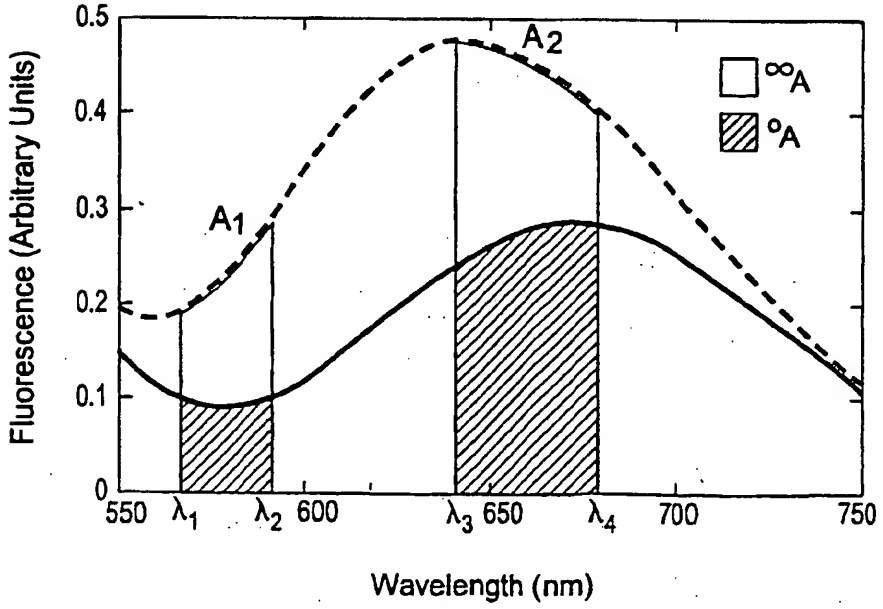
A2
∞A
°A
A1
0.5
0.4
0.3
0.2
0.1
0
550
λ1
λ2
600
λ3
650
λ4
700
750
Fluorescence (Arbitrary Units)
Wavelength (nm)

Fig. 4B

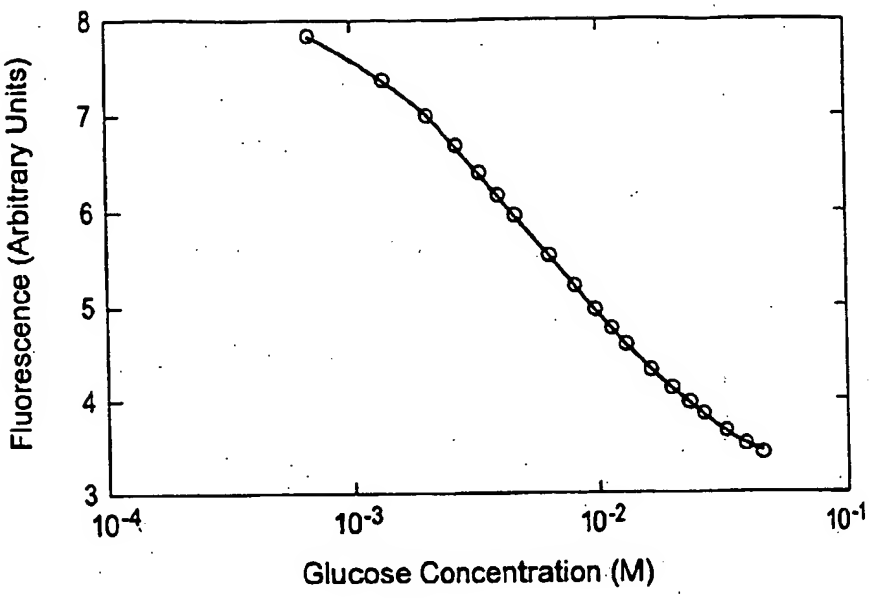
Fluorescence (Arbitrary Units)
8
7
6
5
4
3
10^{-4}
10^{-3}
10^{-2}
10^{-1}
Glucose Concentration (M)

Fig. 5A

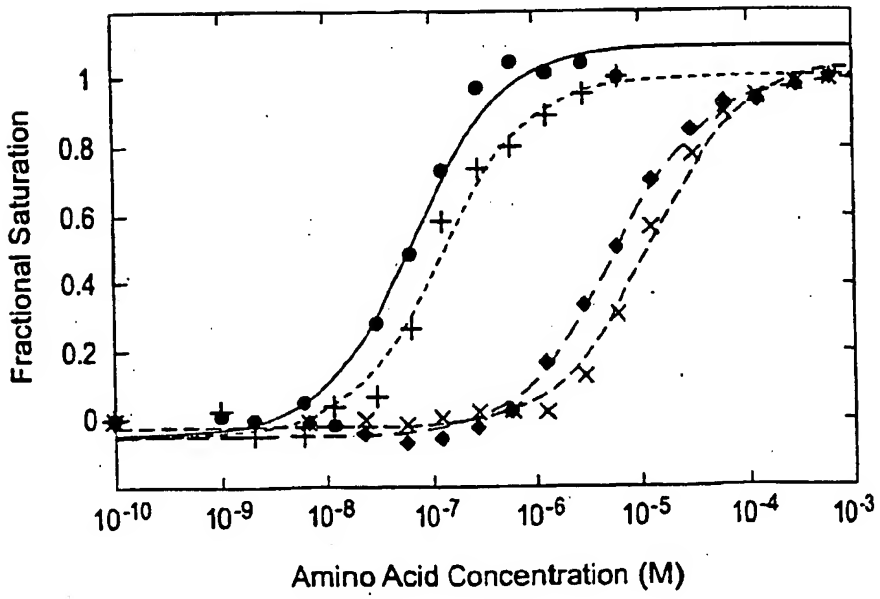
Fractional Saturation
1
0.8
0.6
0.4
0.2
0
10^{-10}
10^{-9}
10^{-8}
10^{-7}
10^{-6}
10^{-5}
10^{-4}
10^{-3}
Amino Acid Concentration (M)

Fig. 5B

Fig. 6A

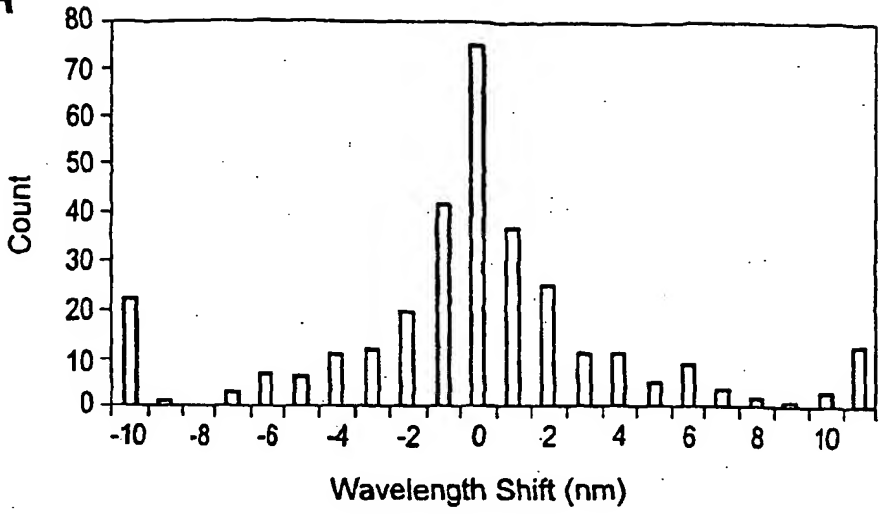

Fig. 6B

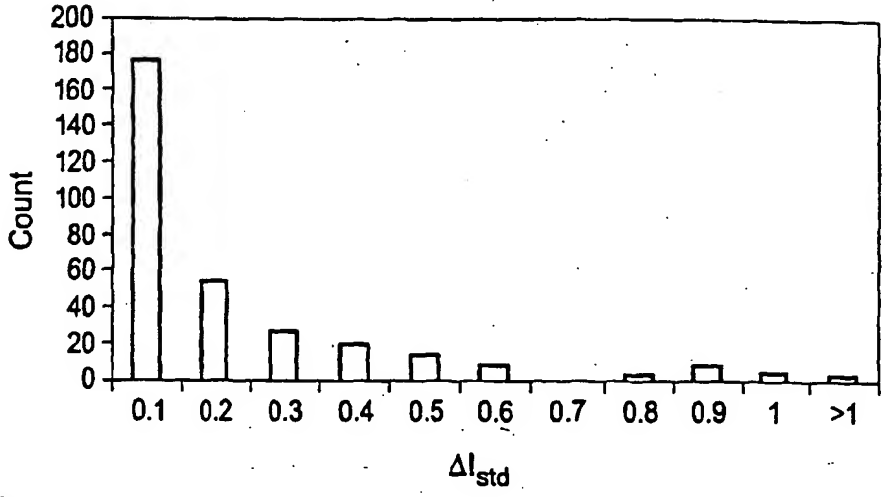

Fig. 6C

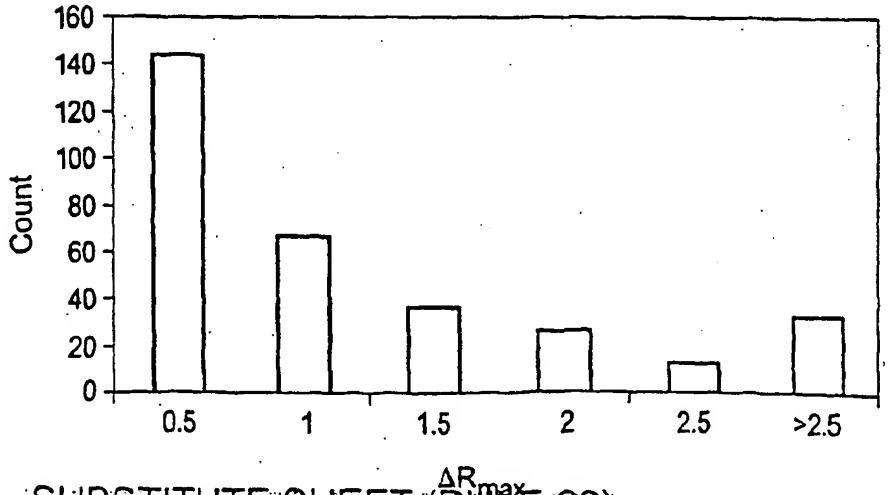

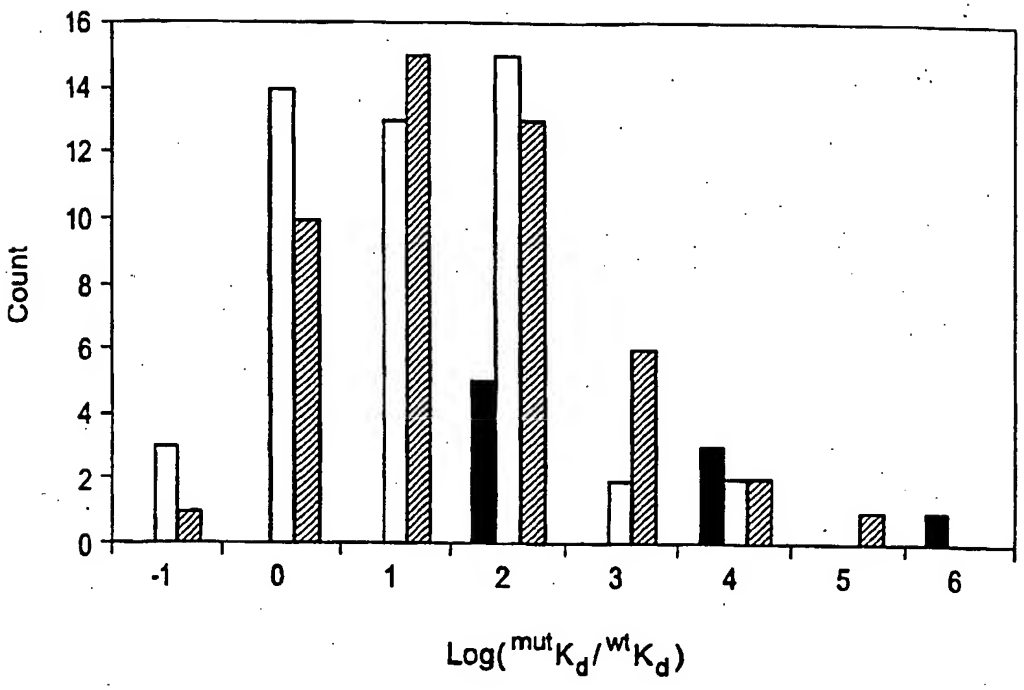

Fig. 7

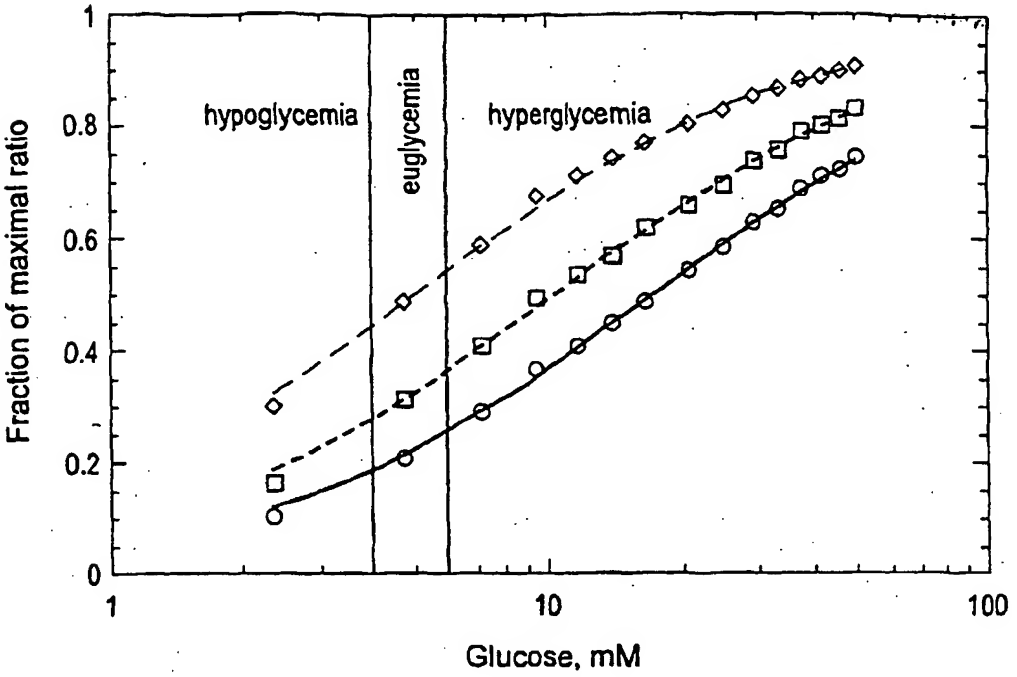
hypoglycemia
euglycemia
hyperglycemia
Fraction of maximal ratio
0
0.2
0.4
0.6
0.8
1
1
10
100
Glucose, mM

Fig. 8A

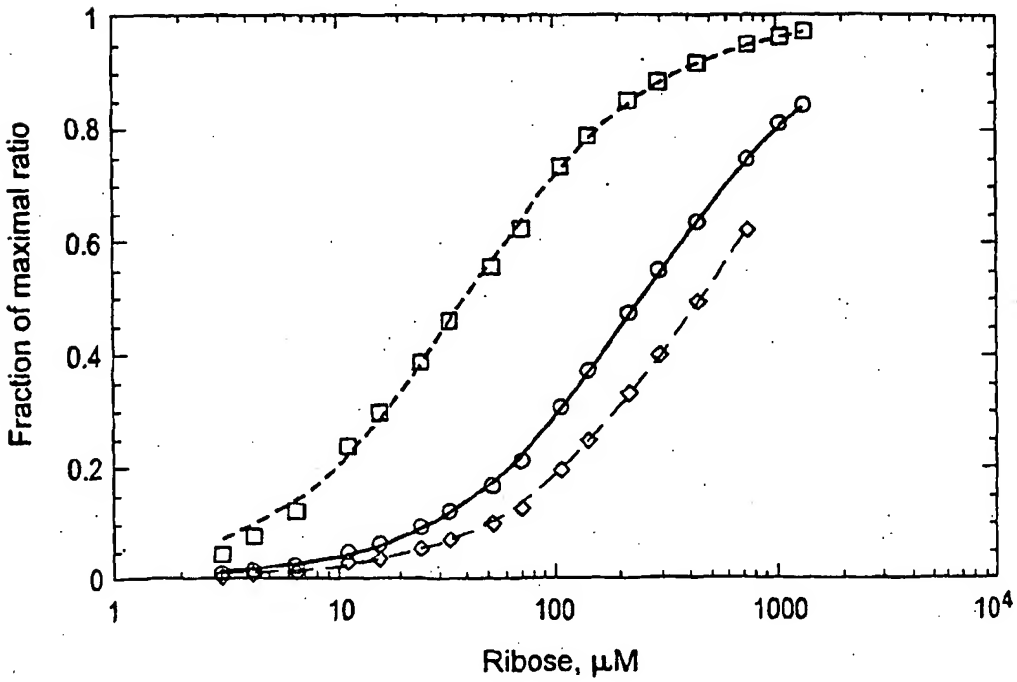
Fraction of maximal ratio
0
0.2
0.4
0.6
0.8
1
1
10
100
1000
10^4
Ribose, µM

Fig. 8B

This Page is Inserted by IFW Indexing and Scanning Operations and is not part of the Official Record

BEST AVAILABLE IMAGES

Defective images within this document are accurate representations of the original documents submitted by the applicant.

Defects in the images include but are not limited to the items checked:

- ☑ BLACK BORDERS
- ☐ IMAGE CUT OFF AT TOP, BOTTOM OR SIDES
- ☐ FADED TEXT OR DRAWING
- ☐ BLURRED OR ILLEGIBLE TEXT OR DRAWING
- ☐ SKEWED/SLANTED IMAGES
- ☑ COLOR OR BLACK AND WHITE PHOTOGRAPHS
- ☐ GRAY SCALE DOCUMENTS
- ☐ LINES OR MARKS ON ORIGINAL DOCUMENT
- ☐ REFERENCE(S) OR EXHIBIT(S) SUBMITTED ARE POOR QUALITY
- ☐ OTHER: _____

IMAGES ARE BEST AVAILABLE COPY.
As rescanning these documents will not correct the image problems checked, please do not report these problems to the IFW Image Problem Mailbox.